MICRO-RNA146B PROMOTES ALVEOLAR PROGENITOR CELL MAINTENANCE THROUGH PREFERENTIAL REGULATION OF STAT3B

By

Hanan Sataa Elsarraj

MD, Tripoli University, 2007

Submitted to the graduate degree program in Pathology and Laboratory Medicine and the Graduate Faculty of the University of Kansas in partial fulfillment of the requirements for the degree of Master of Arts.

_____

Fariba Behbod, Pharm.D., Ph.D.

Chairperson

_____

Roy A. Jensen, M.D.

_____

Timothy A. Fields, M.D., Ph.D.

_____

Lane Christenson, Ph.D.

_____

Nikki Cheng, Ph.D.

_____

Fang Fan, M.D., Ph.D.

Date Defended: July 12, 2012

The Thesis Committee for Hanan Sataa Elsarraj

certifies that this is the approved version of the following thesis:

MICRO-RNA146B PROMOTES ALVEOLAR PROGENITOR CELL MAINTENANCE THROUGH PREFERENTIAL REGULATION OF STAT3B

_____

Fariba Behbod, Pharm.D., Ph.D.

Chairperson

Date approved: July 12, 2012

Abstract:

In this research, we have demonstrated that miRNA146b-5p (miR146b) is a hormonally regulated miRNA that participates in the maintenance of mammary alveolar progenitors during pregnancy and lactation by preferential regulation of STAT3β. Recently, our laboratory isolated distinct ductal, alveolar and multipotent mammary progenitors by single-cell cloning of the COMMA-D (CD) cell line. Molecular characterization of the distinct clones showed significantly higher expression of miR146b in the CD derived alveolar compared to the ductal and multipotent progenitors. Additionally, there was a significant rise in miR146b mRNA levels in the pregnant and lactating mouse mammary glands and in virgin glands following *in vivo* administration of estrogen and progesterone. An analysis of mammary epithelial subpopulations during pregnancy showed a significantly higher expression of miR146b in the alveolar luminal progenitors compared to stem and differentiated luminal cells. Induced knockdown of miR146b led to increased cell death in the CD derived alveolar progenitors and a significant reduction in the percentage of primary mouse mammary alveolar luminal progenitors. Among several of the candidate targets, miR146b regulated STAT3β and to a lesser extent STAT3α. A reporter construct using STAT3α 3'UTR inserted downstream of the firefly luciferase showed a significant reduction in reporter activity when cells overexpressed miR146b. As an imbalance in miR146b has been linked to human breast cancers, regulation of STAT3 isoforms may be a novel mechanism by which miR146b participates in breast carcinogenesis.

Acknowledgements:

I would like to thank Dr. Fariba Behbod, for her enthusiasm, her encouragement, and support throughout the production of this research and thesis. I am also indebted to my committee members, Drs. Timothy Fields, Fang Fan, Nikki Cheng, Lane Christenson and Roy Jensen, for their helpful suggestions and for serving on my thesis committee. I would also like to thank my fellow lab members, past and present: Dr. Kelli Valdez, Yan Hong, Saloumeh Arjmand, Dr. Martha Carletti and Dr. Arindam Paul for their assistance and support and for creating a friendly atmosphere in our lab over the past two years.

I would like to thank Dr. Shane Stecklein and Sally Salah for helping me to get things work, and I thank Richard Hastings and Alicia Zeiger, for flow cytometry technical assistance and guidance.

I would like to acknowledge the NIH 5 R00 CA127462 to FB, The Center of Excellence Fellowship to KV, COBRE Pilot award P20 RR024214 for funding my project, and CBIE-Libyan North American Scholarship Program for funding my Masters training.

I would like to thank my parents, Sataa and Salha, and my sisters, Afaf, Ebtihaj, and Esra for their unwavering support and encouragement throughout the years.

Finally, I would like to thank my loving husband, Ziad, and son, Ayhem, for sticking with me through all the good times and bad, and for never failing to lift my spirit.

Table of Contents:

List of Figures

***Chapter I*: Introduction**

***Chapter II*: Results and Discussion**

***Chapter IV*: Conclusion**

List of Abbreviations

AGO2	Argonaute 2
BRAF	Serine/threonine-protein kinase B-Raf
BRCA1	Breast cancer type 1/2 susceptibility protein
CDβ	Comma D β Cell line
C/ EBPβ	CCAAT/enhancer binding protein-beta
CK5	Cytokeratin 5
CK8	Cytokeratin 8
CSF-1	Colony stimulating factor 1
E	Estrogen
EGF	Epidermal growth factor
EMT	Epithelial-mesenchymal transition
ELF5	E74-like factor 5
ER^+	Estrogen receptor-positive
EXPO5	Exportin 5
FACS	Fluorescence-activated cell sorting
FGF	Fibroblast growth factor
IGF	Insulin-like growth factor
IRAK1	Interleukin (IL)-1 receptor associated kinase
MaSCs	Mammary stem cells
miRNA	Micro-RNA
MiR146b	MicroRNA-146b-5p
MMP16	Matrix metalloproteinase 16
NFkB	Nuclear factor kappa-light-chain-enhancer of activated B cells
NKCC1	Na-K-Cl cotransporter 1
P	Progesterone
pri-miRNA	Primary miRNAs
PRL	Prolactin
PTBP1	Polypyrimidine tract-binding protein 1
RANKL	Receptor activator of nuclear factor kappa-B ligand
RISC	RNA-induced silencing complex
SMA	Smooth muscle actin
SMAD4	SMAD family member 4
STAT3	Signal transducer and activator of transcription 3
STAT5a	Signal transducer and activator of transcription 5a
TGFβ	Transforming growth factor beta
TRAF6	TNF receptor-associated factor 6

Chapter I: Introduction

Prospective isolation and characterization of committed and multipotent progenitors from immortalized mouse mammary epithelial cells with morphogenic potential:

Our knowledge of the components of the mammary epithelial cell hierarchy has expanded in recent years as a result of the development of strategies to prospectively isolate phenotypically distinct subsets of mammary cells using fluorescence-activated cell sorting (FACS) and assessing the properties of these cells using *in vitro* and *in vivo* functional assays.

Mammary stem cells (MaSCs) are presumed to be important for both mammary development and maintaining tissue homeostasis. The cells give rise to mature epithelium of either the luminal or myoepithelial lineage via a series of lineage-restricted intermediates. The luminal lineage can be further subdivided into ductal cells that line the ducts, and alveolar luminal cells that constitute the alveolar units which arise during pregnancy. In contrast, myoepithelial cells are specialized, contractile cells located at the basal surface of the epithelium adjacent to the basement membrane [1]. In general, the stem cells are thought to give rise to committed progenitor cells for either the myoepithelial or luminal epithelial lineages (ductal and alveolar sublineages), but the precise number and nature of the intermediates remain elusive [1]. A hypothetical model has been proposed by Kittrell et al. [2] where the mammary epithelial cell hierarchy begins with asymmetric self-renewal in the stem cells, which generate multipotent and bipotent ductal and alveolar progenitor cells. Ductal and alveolar progenitor cells give rise to luminal and myoepithelial-restricted progenitors (Fig.1), which then form the differentiated luminal and differentiated myoepithelial cells respectively. The observation of epithelial outgrowths with either ductal-only or alveolar-only characteristics that contain both luminal and myoepithelial elements following mammary cell transplantation lends support to this model.

Previous studies define the subpopulations enriched in stem cells by the expression of unique surface markers, lineage-negative (lin^-) $CD24^+CD29^{high}$ and $lin^-CD24^+CD49f^{high}$, luminal

progenitors by $lin^{-}CD29^{low}CD24^{+}CD61^{+}$, differentiated estrogen receptor-positive (ER^{+}) luminal cells by $CD24^{+}CD133^{+}$ and myoepithelial progenitors by $CD29^{low}CD24^{low}$ [3,4,5]. Regan et al. [6] showed that the c-Kit signaling pathway is required for the normal function of mammary epithelial progenitors. In this study, $CD24^{+/Low}$ $Sca\text{-}1^{-}$ $CD49f^{Low}$ was demonstrated to represent a marker for for the myoepithelial cells, $CD24^{+/Low}$ $Sca\text{-}1^{-}$ $CD49f^{High}$ for the mammary stem cells, $CD24^{+/High}$ $Sca\text{-}1^{-}$ for the luminal ER- progenitor cells, and $CD24^{+/High}$ $Sca\text{-}1^{+}$ for luminal differentiated ER+ cells. Additionally, this study, demonstrated that the majority of luminal ER- progenitors are c-Kit+, but also most stem cells and the differentiated cell populations are c-Kit+ [6].These studies facilitated the analysis of the mammary epithelial subpopulations, which is a key for understanding mammary epithelial stem/progenitor cells in normal tissue biology and carcinogenesis.

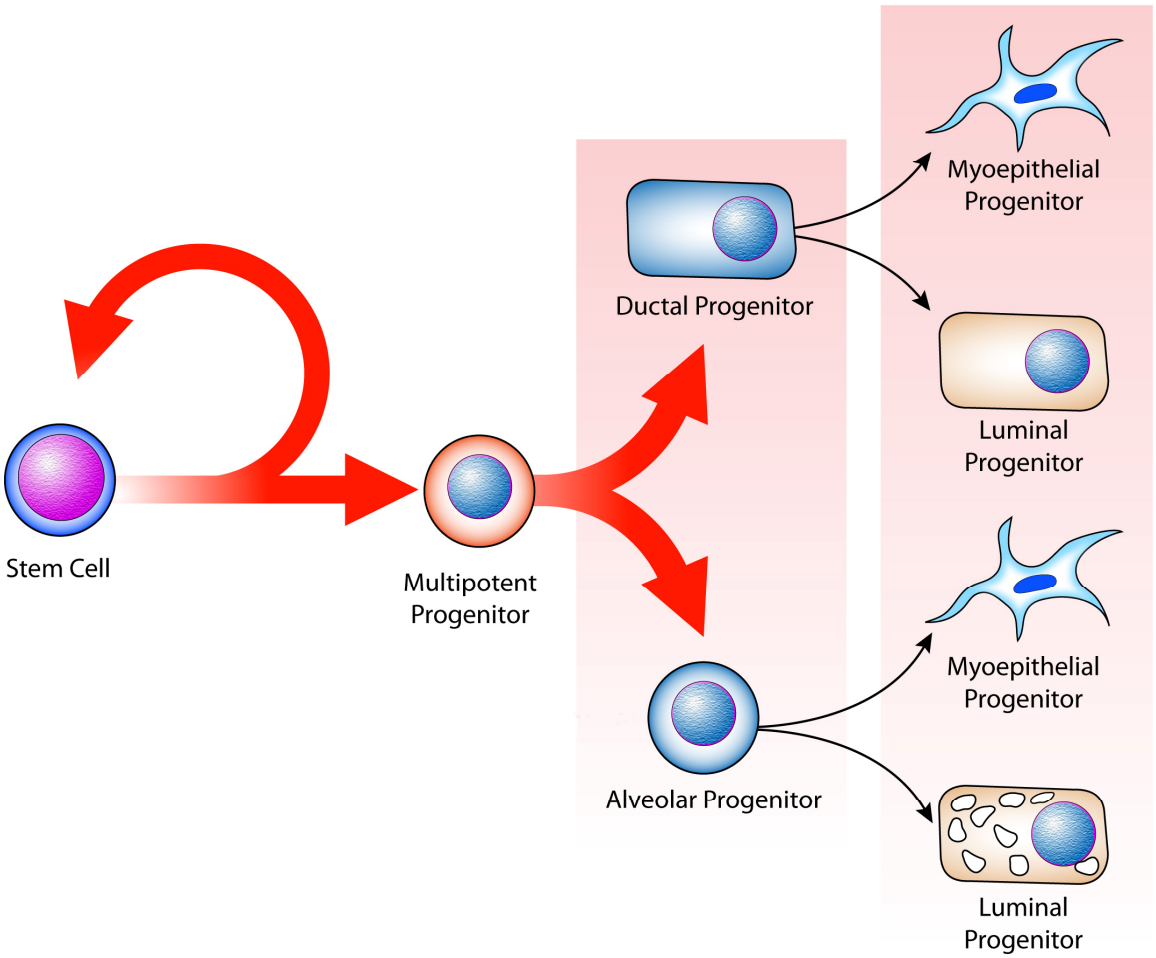

Figure.1: Hypothetical model of stem cell differentiation during mammary gland development. Mammary gland development begins by asymmetric self-renewal in a stem cell, which generates multipotent and bipotent ductal and alveolar progenitor cells [2].

Using single-cell cloning, Dr. Behbod's laboratory isolated distinct mammary progenitor populations from the CD cell line, which was originally derived from mid-pregnancy BALB/c mouse mammary glands. This cell line is unique in that transplantation of cells into the epithelium-free fat pads of syngenic female mice generates mammary ductal and alveolar structures.

In this study, CDβ cells were stained using Hoechst dye 33342, followed by FACS analysis and sorting of each population. Cells that effluxed the dye appeared on the left side of a FACS analysis panel were referred to as side population "SP" cells. This elevated rate of Hoechst efflux was previously suggested as being due to expression of the Adenosine Binding Cassette (ABC) trans-membrane pump (Abcg2) which pump vital dyes out of cells [7]. Cells that retained the dye appeared on the right side and were referred to as non-side population "NSP" cells. To assess the stem progenitor cell potential of the SP cells compared to the NSP cells, single cells were sorted from each region, expanded *in vitro* and transplanted to assess their outgrowth potential. As shown, in (Fig. 2), Transplantation of the SP3 clone generated only alveolar structures *in vivo* and is referred to herein as an "alveolar progenitor clone". Transplantation of NSP2 generated only ductal structures and is referred to herein as a "ductal progenitor clone". Transplantation of clones NSP1 and NSP5 generated ducts and alveolar structures and are referred to herein as "multipotent progenitor clones". Stimulation of mice transplanted with cells from the "alveolar progenitor" and the "ductal progenitor" clones with pituitary isografts results in formation of milk droplets in the alveolar progenitor clone, in contrast to the ductal progenitors, which don't make milk but produces intraductal hyperplasia. Pituitary isografts release pregnancy hormones including E+P and prolactin. Furthermore, the

clones' outgrowths showed an appropriate basal-luminal orientation with a basal expression of SMA, CK5 and p63, and luminal expression of CK8 and NKCC1.

These distinct progenitor clones have been utilized as an experimental tool in this thesis, to further investigate the molecular mechanisms involved in mammary lineage maintenance and commitment.

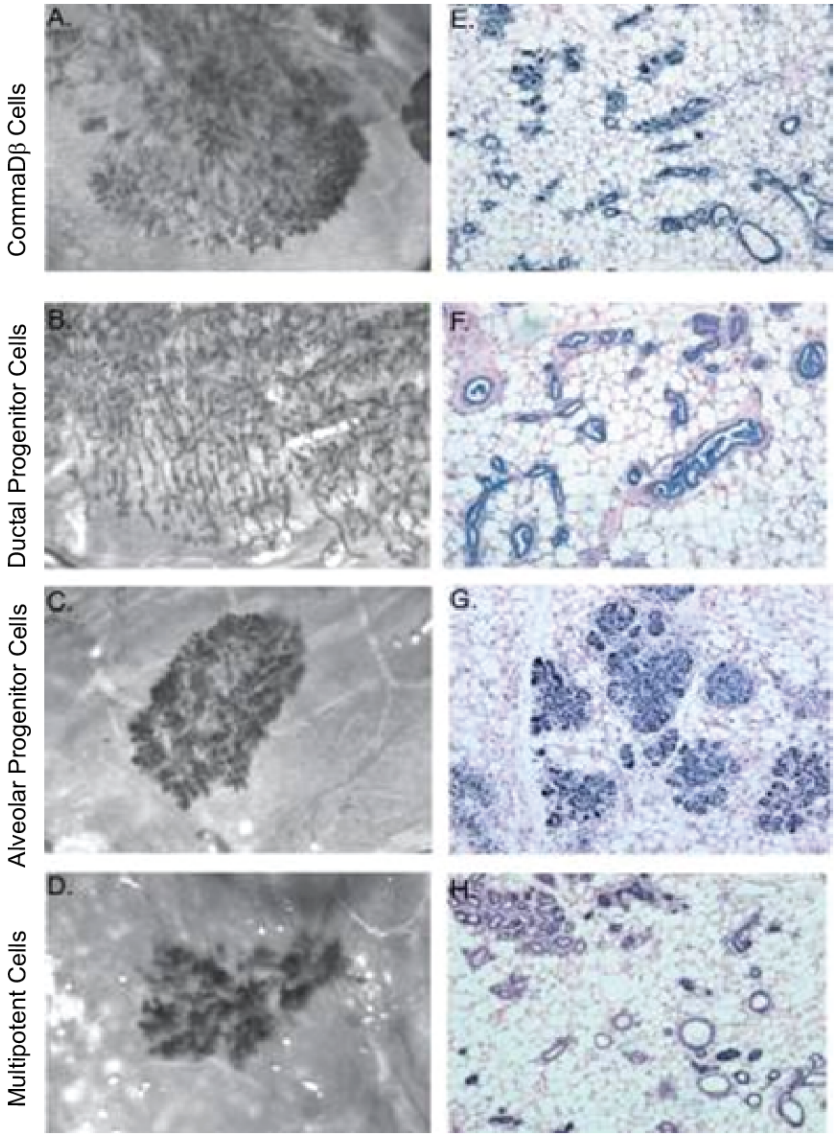

Figure. 2 Whole-mount and hematoxylin and eosin staining of outgrowths generated from the CDβ parental line and CDβ progenitor clones. **(A and E)** Transplantation of COMMA-D cell line engineered to express β-galactosidase (CDβ) parental cell line generates outgrowths containing ductal and alveolar structures. **(B and F)** Ductal progenitor cells give rise to outgrowths containing ducts only. **(C and G)** Alveolar progenitor clone generates mainly alveoli and a limited number of small ducts. **(D and H)** Multipotent progenitor clone generates outgrowths containing ductal and alveolar structures. Figures 2A to 2D are whole-mount-stained images taken at 3.2x original magnification. Figures 2E to 1H are hematoxylin and eosin-stained images taken at 10x original magnification [2].

Mammary gland development

The development of mammary gland is a highly dynamic process and involves the distinct stages of embryonic, pubertal, pregnancy, lactation and involution. Hormones and growth factors play a role in these different stages of mammary development and also implicated in breast cancer [8]. During pregnancy, the hormone progesterone (P) in combination with prolactin (PRL) induce alveolar proliferation (lactogenesis I), the functional differentiation and milk secretion are achieved shortly before parturition (lactogenesis II) [8]. Lactation requires the production of specific cells that can synthesize and secrete copious amounts of milk. At the end of the lactation period, the mammary alveolar compartment regresses rapidly, and the morphology of the gland resembles that of a mature virgin. It is generally agreed that during involution, the differentiated alveolar cells undergo apoptosis, and that the alveolar compartment is reconstituted in subsequent pregnancies from undifferentiated mammary stem cells or alveolar precursors [9].

Hormonal regulation of alveolar differentiation: In the late fifties, a series of experiments defined the minimal hormonal requirements for mammary gland development in mice [10], and rats [11]. Hormone replacement in animals that have been hypophysectomized, ovariectomized, and adrenalectomized established that additive and sequential treatment with 17-b-estradiol, progesterone, and prolactin in conjunction with cortisol and GH can recapitulate mammary gland development. Furthermore, findings indicate that estrogen can target the stromal and epithelial compartments of the mammary gland, progesterone can target the epithelium, and prolactin can target the epithelium and potentially the stroma [12]. Since most cells that proliferate in response to estrogen treatment *in vivo* do not contain estrogen receptors, it is possible that estrogen might

probably have indirect mechanisms, which include the induction of local growth factors or their receptors [12].

Genetic Pathways Controlling Mammary Development: Among the growth factors that have demonstrated roles, or are highly implicated, in mammary growth and differentiation are the EGF, TGF-β, FGF, and IGF families [13]. Ductal elongation and branching during puberty is controlled by inhibinβ, CSF-1, the progesterone and estrogen receptor, and wnt. Proliferation and differentiation of mammary alveolar cells is controlled by the prolactin receptor, STAT5, RANKL, cyclinD1, p27, Id2, and C/EBPβ. Mammary function during lactation is controlled by prolactin through STAT5, and tissue remodeling and cell death during involution by STAT3, bax, and bcl-x [14]. Among these factors, we focused on STAT3 and STAT5a due to their established role in alveolar development and remodeling.

Signal transducer and activator of transcription 3 (STAT3) in mammary gland development and cancer

Signal transducer and activator of transcription 3 (STAT3) is a member of the STAT family of transcription factors implicated in growth factor and cytokine signaling. STAT3 exists in two main isoforms: full-length STAT3α and truncated STAT3β; the proteins are generated by alternative mRNA splicing of exon 23 [15,16]. In STAT3β, the 55-amino acid C-terminal acidic transactivation domain of STAT3α is replaced by seven unique amino acid residues (CT7 domain) (Fig. 3) [16]. STAT3β has been known to function as a dominant-negative factor by inhibiting STAT3α gene transactivation [17,18]. However, more recent studies have demonstrated that STAT3β to serve as more than just a dominant-negative regulator, since it activates a specific set of genes and possesses non-redundant functions to

STAT3α. Furthermore, STAT3β over-expression induces apoptosis in some breast cancer cell lines [17].

During mammary gland development, it has become clear that STAT3 regulates a complex series of processes involving alveolar epithelial cell death during involution by maintaining the balance of inflammatory and anti-inflammatory signaling [19], and mice with a mammary-specific conditional deletion of STAT3 exhibit a notable delay in this process [20]. The contribution of specific STAT3 isoforms to mammary involution process is still not known. However, in this study we clearly demonstrate that both isoforms of STAT3 are up-regulated during involution. It would be interesting to decipher the contribution of specific STAT3 isoforms to the mammary involution process.

In breast cancer, STAT3 has been classified as an oncogene because the constitutively active STAT3 can mediate oncogenic transformation in cultured cells and tumor formation in nude mice [21]. Moreover, a number of independent studies have reported that the majority of primary breast cancers exhibit a constitutive activation of STAT3 and that this particular signal transducer plays an important role in breast cancer cell growth and metastatic progression [21,22,23,24]. Therefore, functional inhibition of STAT3 as part of a targeted therapy for advanced breast cancers may prevent the metastatic dissemination of malignant cells [25].

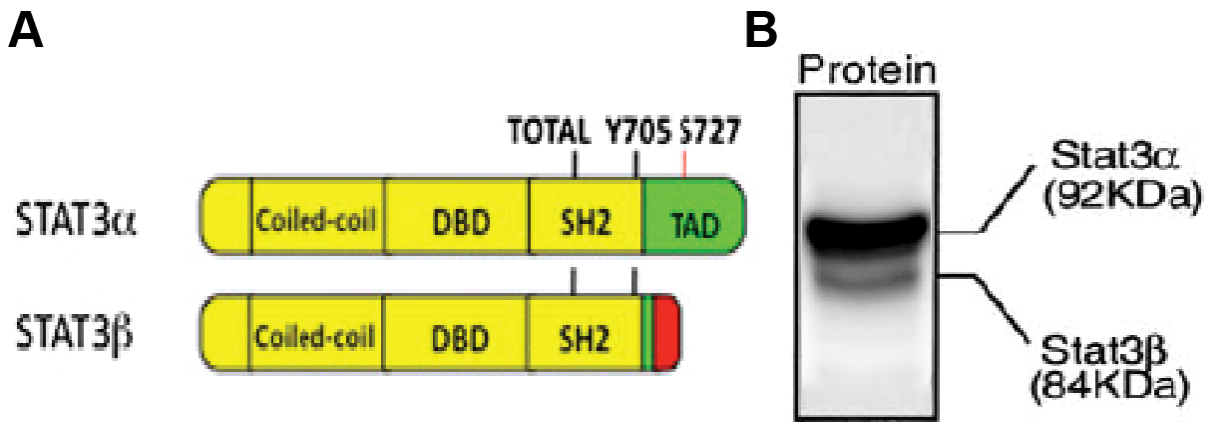

Figure. 3 Differences in STAT3α and STAT3β structure. A: Alternative 3' splice site use in exon 23 generates STAT3α or STAT3β, where the TAD (green) is substituted by a unique 7-aa tail (red). DBD, DNA binding domain. STAT3β can be efficiently be phosphorylated at the key tyrosine 705 (Y705) but lacks serine 727 (S727) [16], whose phosphorylation stimulates transcriptional activity. B: Immunoblotting with a pan-specific STAT3 antibody detects STAT3α and STAT3β in mammary epithelial cell lysates.

MicroRNAs:

MicroRNAs (miRNAs) are a specific class of endogenous non-coding RNAs that are typically conserved across species. They are single-stranded RNAs of 21-25 nucleotides in length, and function in post-transcriptional gene silencing [26].

The biogenesis of miRNAs (Fig. 4) begins by RNA polymerase II. Primary miRNAs (pri-miRNA) are produced from miRNA genes which contain their own promoters, whereas mirtrons are formed from splicing stem-loop structures present in pre-mRNA transcripts. Both of these classes undergo additional processing to form precursor miRNAs (pre-miRNA), with pri-miRNAs requiring the RNase III enzyme Drosha, and the mirtron-derived lariat structures employing the lariat-debranching enzyme (DBR1). Exportin 5 (EXPO5) shuttles pre-miRNAs to the cytoplasm, at which point they are processed into mature miRNAs by another RNase III enzyme, Dicer. The dsRNA binding protein (TRBP) binds to Dicer and loads the miRNA into the Argonaute 2 (AGO2) endonuclease. The Dicer-TRBP-AGO2 complex, referred to as RNA-induced silencing complex (RISC), directs complementary binding of miRNAs to target mRNAs (generally in the 3′ untranslated region of the mRNA), and facilitates translational repression by promoting mRNA degradation or preventing translation initiation [26]. MiRNAs may regulate targets cooperatively, and many demonstrate remarkable promiscuity, targeting several or even hundreds of mRNAs [27].

MiRNAs have been experimentally linked to both normal physiology and pathology, including regulation of developmental processes, proliferation, differentiation and apoptosis. Loss of mature miRNAs resulted in a failure of the cells to differentiate [28,29,30,31], providing evidence that miRNAs may also be involved in maintaining stem cell populations by keeping

them in an undifferentiated state, controlling stem cell self-renewal and regulating the transition of undifferentiated stem cells to more differentiated states [26].

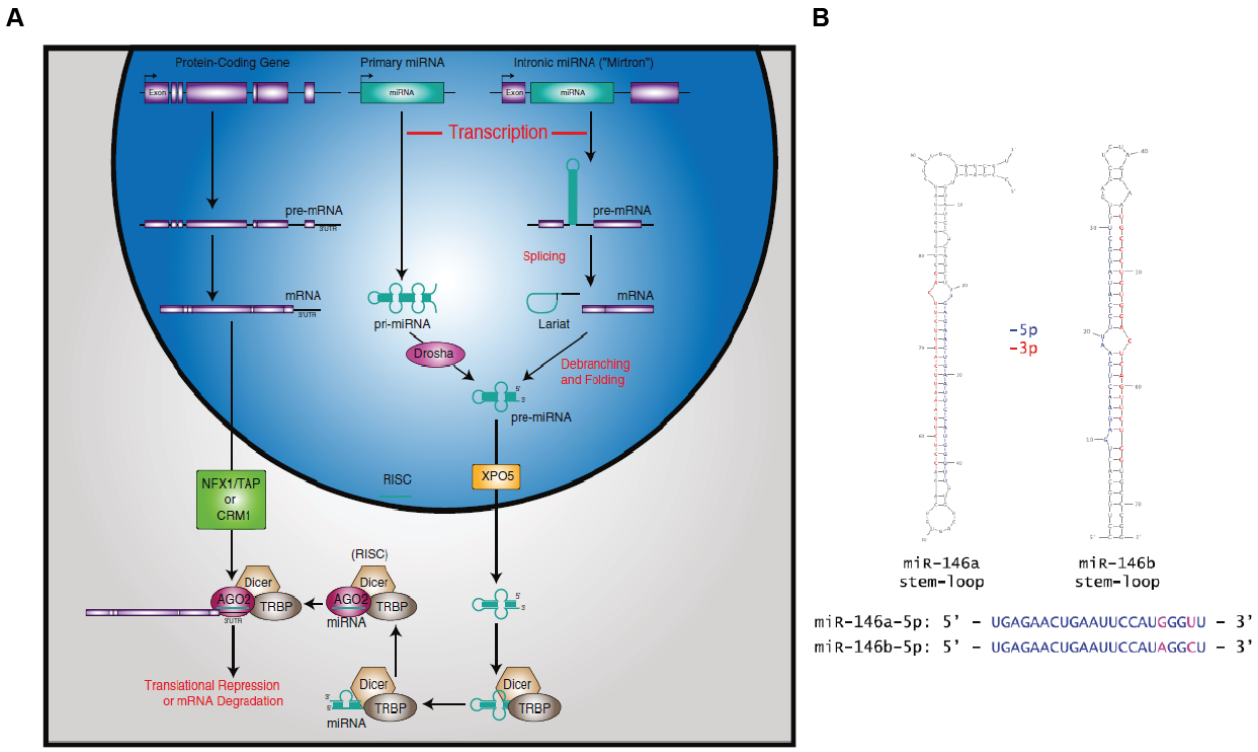

Figure.4: A, Biogenesis and function of miRNAs. MiRNAs are transcribed as primary miRNAs (pri-miRNA) or are derived from stemloop structures "Mirtrons" within pre-mRNAs. Drosha processes pri-miRNAs whereas the stem-loop-derived structures depend on the lariat-debranching enzyme (DBR1) to form precursor miRNAs (premiRNAs). Exportin 5 (XPO5) exports pre-miRNAs into the cytoplasm where they are further processed by the Dicer/TRBP complex into mature miRNAs. Argonaute 2 (AGO2) joins the Dicer/TRBP complex to generate the RNA-induced silencing complex (RISC) which mediates binding to complimentary sequences in target mRNAs and translational repression or mRNA degradation. **B, Structure of miR-146a/b.** Predicted stem-loop structures of miR-146a and miR-146b. The mature miR-146a-5p and miR-146b-5p differ by only two bases in the 3'region [32].

MiR146a/b in development and cancer:

Mouse miR146b is located on chromosome 19 at position 19qC3 whereas miR146a is located on chromosome 11 at position 11qA5 [33]. Structurally, the mature miR146a and miR146b differ by only two nucleotides at the 3' end, a region that is believed to play a minor role in target recognition, and in many instances miR146a and miR146b have demonstrated redundant activities [34]. Mice knockout for miR146a exhibit increased sensitivity to LPS [35,36]. Older knockout animals were also noted to have a significantly increased risk of malignant hematolymphoid neoplasia [36]. Interestingly, estrogen stimulation has been reported to downregulate the expression of miR146a in splenic lymphocytes and as such miR146a may play a role in down-modulating LPS mediated immune responses [37]. As of the writing of this manuscript, a miR146b knockout mouse has not been reported.

There are conflicting reports on the role of miR146a/b in cancer progression. A study by He, H. et al. showed that three miRNAs (miR146, miR221, and miR222) were dramatically overexpressed in papillary thyroid cancers (PTC) compared to the adjacent unaffected thyroid tissue [38]. This group concluded that among tumors with BRAF mutations, overexpression of miR146b was associated with aggressive behavior in PTC tumors. Bockmeyer et al. [39], studied the microRNA profiles of healthy basal and luminal epithelial cells as well as basal and luminal breast cancers. Interestingly, miR146b was shown to be a basal-specific microRNA and to be expressed at higher levels in basal-like breast cancers compared to luminal A and B subtypes [39]. Garcia et al. [40] studied the regulation of BRCA1 by the miR146 family, and found that miR146a and miR146b expression to be higher in basal-like breast cancer cell lines, a subtype which commonly exhibits low or absent BRCA1 expression [41,42]. They also showed that miR146a and miR146b precursor transfection increased cell proliferation in HeLa and in

MDA-MB-468 cells by targeting the 3'UTR of BRCA1 and down-regulating its expression. Furthermore, both miR146a and miR146b were upregulated in triple negative versus ER+/PR+, and in the Scarff-Bloom-Richardson (SBR) grade III versus grade II breast tumors [40]. Based on this work, miR146a/b may play a role in breast cancer progression. Conversely, miR146b has also been shown to inhibit carcinogenesis. For example, miR146b was shown to inhibit glioblastoma cell migration and invasion by targeting matrix metalloproteinase 16 (MMP16), a protease selectively expressed in the brain [43]. Welch and colleagues [44]recently coined the term "metastamir" to refer to metastasis regulatory miRNAs that have an impact on critical steps in the metastatic cascade, such as epithelial-mesenchymal transition (EMT), apoptosis, and angiogenesis [44]. This group has classified miR146a/b as a "metastasis-suppressing metastamir"[44]. Bhaumik et al. demonstrated that over-expression of miR146a/b in the highly metastatic human breast cancer cell line MDA-MB-231 caused suppression of constitutive NF-κB activity by down-regulating IRAK1 and TRAF6, two key adaptor/scaffold proteins in the IL-1 and TLR signaling pathway known to positively regulate NF-κB activity [45]. Furthermore, miR146a/b-expressing cells displayed only 45% and 38% of the control migration capacity, respectively. Interestingly, although compromised in their motility and invasiveness, miR146a/b-overexpressing cells exhibited no proliferation impairment or apoptosis sensitivity relative to control cells [45]. Another study by Hurst et al. [44] revealed that breast cancer metastasis suppressor 1 (BRMS1), a nuclear protein that causes suppression of cancer metastasis, could exert its anti-metastatic action by differentially regulating expression of miR146a and miR146b. In addition, both miR146a/b reduced EGFR expression and suppressed metastasis [44]. These findings suggest that miR146a/b may play a dual role in cancer and there is much to

be learned about the mechanism by which these closely related miRNAs may participate during various stages of carcinogenesis.

In this study, we have identified a hormonally regulated miRNA, miR146b, that plays a pivotal role in alveolar progenitor cell maintenance. Altered expression of miR146b has been linked to an invasive and metastatic capacity in diverse cancers. Finding a hormonally regulated miRNA that regulates both the processes of alveolar cell maintenance and breast cancer may provide a missing link in the molecular pathways implicated in hormonal regulation of human breast cancer.

Chapter II: Results and Discussion

MiR146b is highly expressed in the alveolar progenitor cells

As described in the introduction, distinct mammary alveolar, ductal and multipotent progenitor clones were derived from the CD cell line [2]. An RT2 miRNA PCR array was used to screen the specific CD derived clones to screen for changes in the expression of 84 unique miRNAs, (Fig. 1A). This screening showed a set of 74 up-regulated miRNAs in the clones with *in vivo* growth potential (including the alveolar progenitor, ductal progenitor and multipotent progenitors) when compared to clones that exhibited no in vivo growth potential. Twenty miRNAs showed a 10 to 20-fold increase, and 14 miRNAs showed > 20-fold increase (Fig. 1A). Among those upregulated, miR146b showed >72-fold increase, and miR-203 showed >77-fold increase. To identify whether miR146b, miR203 and other up-regulated miRNAs were differentially expressed in the specific progenitor cell clones, RT-qPCR was used on RNA derived from progenitor clones grown on Matrigel in three dimension (3D). MiR146b was the only miRNA that showed differential expression as it was highly expressed by the alveolar progenitor clone with a 10-fold (± 1.8 SEM) increase compared to the ductal and the multipotent progenitor clones (Fig. 1B), while others such as miR203 expression showed no difference between the distinct progenitor clones (data not shown).

To confirm our findings, we used primary mammary epithelial cells (PMEC) isolated from female balb/c mice during the various stages of mammary development. Mammary epithelial cells were isolated from virgin, pregnant, lactating and 10 days post-weaning (involuting). RT-qPCR showed a 3.5 (6.1± 0.57 SEM vs. 2.3± 0.76 SEM) fold increase in miR146b expression in the PMEC of pregnant and a 6.3 (10.8± 1. 03 SEM vs. 2.3± 0.76 SEM) fold increase in lactating mice compared to PMEC from virgin and post-weaning mice (Fig. 1C). Because the pattern of expression of miR146a and miR146b is similar and the isoforms are co-regulated in normal

mammary cell lines and in breast cancer cell lines [40], RT-qPCR was used to examine miR146a levels as well. The results showed that miR146a levels increased similarly during pregnancy and lactation. However, the fold changes in miR146a during mammary development were not as great as those of miR146b (Fig. 1C).

Recently, the progenitor and differentiated cells in the mouse mammary glands and human breast were phenotypically and functionally characterized by fluorescence-activated cell sorting (FACS) followed by transplantation. These studies define the subpopulations enriched in stem cells by the expression of unique surface markers, lineage-negative (lin-) CD24+CD29high and lin-CD24+CD49fhigh, luminal progenitors by lin-CD29lowCD24+CD61+, differentiated estrogen receptor-positive (ER+) luminal cells by CD24+CD133+ and myoepithelial progenitors by CD29lowCD24low [3,4,5]. To find the mammary epithelial sub-population with the highest miR146b expression, the luminal progenitors (lin-CD29lowCD24+CD61+), stem cells (lin-CD29highCD24+), and differentiated luminal cells (lin-CD29lowCD24+CD61-) were sorted from the balb/c mouse mammary glands during pregnancy, followed by RNA extraction and RT-qPCR for miR146b expression. The results revealed that miR146b expression levels were 3.4-fold (11.8±0.59 SEM) higher ($p<0.05$) in the luminal progenitors compared to the stem cells (3.4±0.87 SEM) and 1.3-fold higher ($p=0.05$) compared to the differentiated luminal cells (9.0±0.47 SEM) (Fig.1D & E). These data supported the earlier results that CD derived alveolar progenitor cells express significantly higher levels of miR146b. In summary, miR146b levels rise during lactation and pregnancy. Since expression was significantly higher in the luminal alveolar progenitor and differentiated luminal cells compared to stem cells, miR146b may play a functional role in these cells.

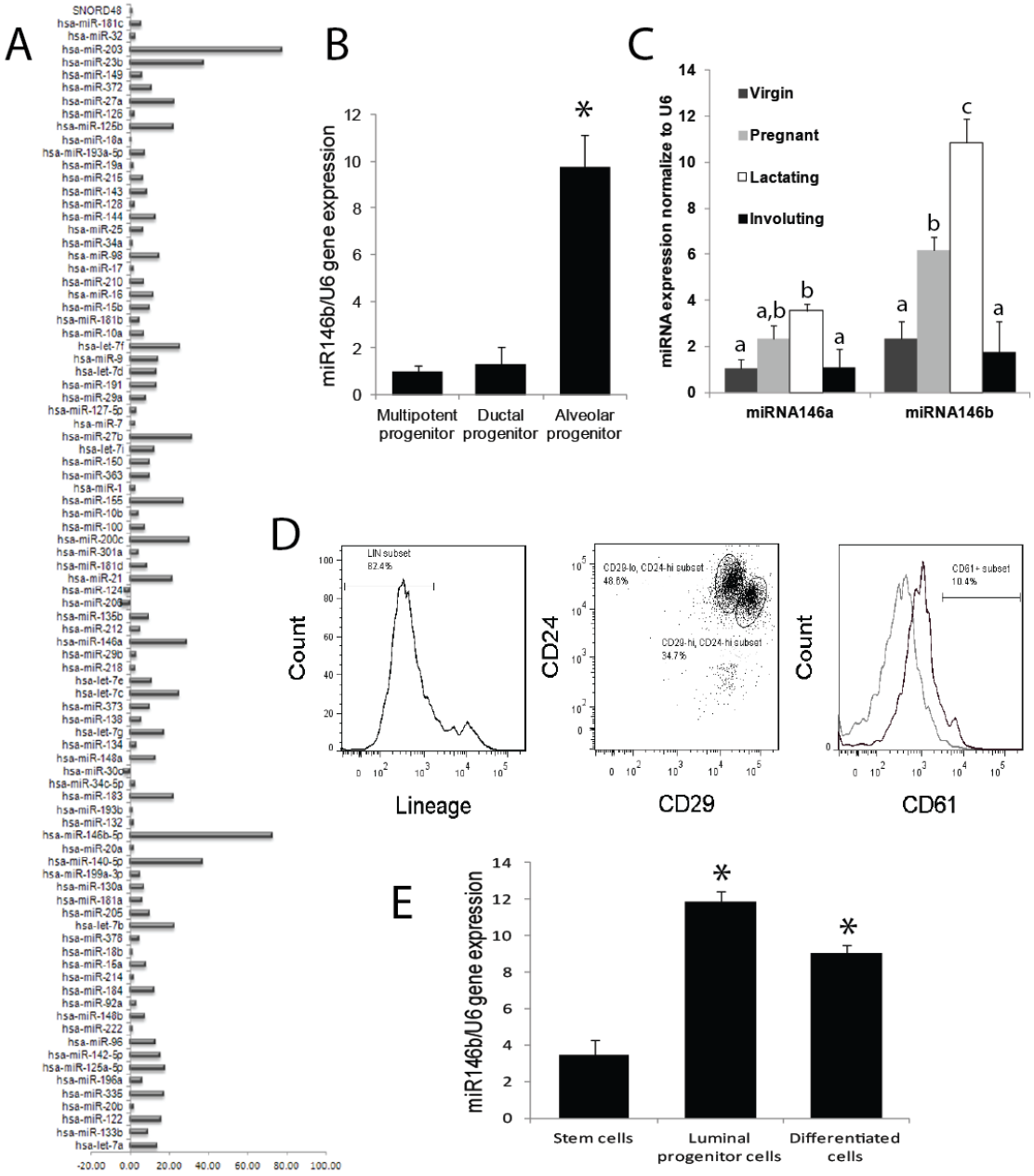
A
SNORD48
hsa-miR-181c
hsa-miR-32
hsa-miR-203
hsa-miR-23b
hsa-miR-149
hsa-miR-372
hsa-miR-27a
hsa-miR-126
hsa-miR-125b
hsa-miR-18a
hsa-miR-193a-5p
hsa-miR-19a
hsa-miR-215
hsa-miR-143
hsa-miR-128
hsa-miR-144
hsa-miR-25
hsa-miR-34a
hsa-miR-98
hsa-miR-17
hsa-miR-210
hsa-miR-16
hsa-miR-15b
hsa-miR-181b
hsa-miR-10a
hsa-let-7f
hsa-miR-9
hsa-let-7d
hsa-miR-191
hsa-miR-29a
hsa-miR-127-5p
hsa-miR-7
hsa-miR-27b
hsa-let-7i
hsa-miR-150
hsa-miR-363
hsa-miR-1
hsa-miR-155
hsa-miR-10b
hsa-miR-100
hsa-miR-200c
hsa-miR-301a
hsa-miR-181d
hsa-miR-21
hsa-miR-124
hsa-miR-200
hsa-miR-135b
hsa-miR-212
hsa-miR-146a
hsa-miR-29b
hsa-miR-218
hsa-let-7e
hsa-let-7c
hsa-miR-373
hsa-miR-138
hsa-let-7g
hsa-miR-134
hsa-miR-148a
hsa-miR-30c
hsa-miR-34c-5p
hsa-miR-183
hsa-miR-193b
hsa-miR-132
hsa-miR-146b-5p
hsa-miR-20a
hsa-miR-140-5p
hsa-miR-199a-3p
hsa-miR-130a
hsa-miR-181a
hsa-miR-205
hsa-let-7b
hsa-miR-378
hsa-miR-18b
hsa-miR-15a
hsa-miR-214
hsa-miR-184
hsa-miR-92a
hsa-miR-148b
hsa-miR-222
hsa-miR-96
hsa-miR-142-5p
hsa-miR-125a-5p
hsa-miR-196a
hsa-miR-335
hsa-miR-20b
hsa-miR-122
hsa-miR-133b
hsa-let-7a
-20.00 0.00 20.00 40.00 60.00 80.00 100.00
B
miR146b/U6 gene expression
Multipotent progenitor
Ductal progenitor
Alveolar progenitor
C
miRNA expression normalize to U6
Virgin
Pregnant
Lactating
Involuting
miRNA146a
miRNA146b
D
LIN subset
82.4%
Count
Lineage
CD29-lo, CD24-hi subset
48.6%
CD29-hi, CD24-hi subset
34.7%
CD24
CD29
CD61+ subset
10.4%
Count
CD61
E
miR146b/U6 gene expression
Stem cells
Luminal progenitor cells
Differentiated cells

Figure 1. MiR146b expression is upregulated in the CD derived alveolar progenitor cells and in mouse mammary glands during pregnancy and lactation. (*A*) An RT^2 miRNA PCR array was used to screen for miRNAs differentially expressed in CD clones with in vivo growth potential normalized to CD clones lacking in vivo growth potential. (*B*) Quantitative PCR of miR146b expression in three CD derived clones grown for 7 days on Matrigel®. Ductal and alveolar progenitor clones were normalized to the multipotent clone (n=4; * indicates $P<0.05$). (*C*) Quantitative PCR of miR146b and miR146a expression in PMECs from mice which were virgin, pregnant, lactating, or 10 days post-weaning (n=3; letters indicate treatment groups which differ, $P<0.05$). (*D*) Representative histograms of the three mammary subpopulations $lin^-CD24^+CD29^{hi}$ (stem cells), $lin^-CD24^+CD29^{lo}CD61^+$ (luminal progenitor cells) and $lin^-CD24^+CD29^{lo}CD61^-$ (differentiated luminal cells) analyzed in the epithelial population from the mammary glands of pregnant mice. The subpopulations were sorted by FACS, and (*E*) analyzed for miR146b expression by qPCR (n=2, * indicates $P<0.05$ compared to the stem cells). Data is presented as the mean ± S.E.M.

Hormonal stimulation results in the upregulation of miR146b in the mammary epithelial cells *in vivo*

To further investigate the influence of steroid hormones on miR146b expression levels, we exposed virgin PMEC to estrogen (E) and progesterone (P) *in vivo.* E + P hormonal pellets were inserted subcutaneously in virgin balb/c mice for three weeks. Following treatment, the mammary glands were removed followed by PMEC isolation. RT-qPCR revealed that E + P treatment resulted in a 4.6-fold (4.6± 0.09 SEM) increase ($p<0.05$) in miR146b expression levels compared to the non-treated controls (Fig. 2). These data demonstrate that the expression of miR146b is regulated by sex hormones. It is still unclear whether regulation of miR146b is a direct or indirect response to hormonal stimulation.

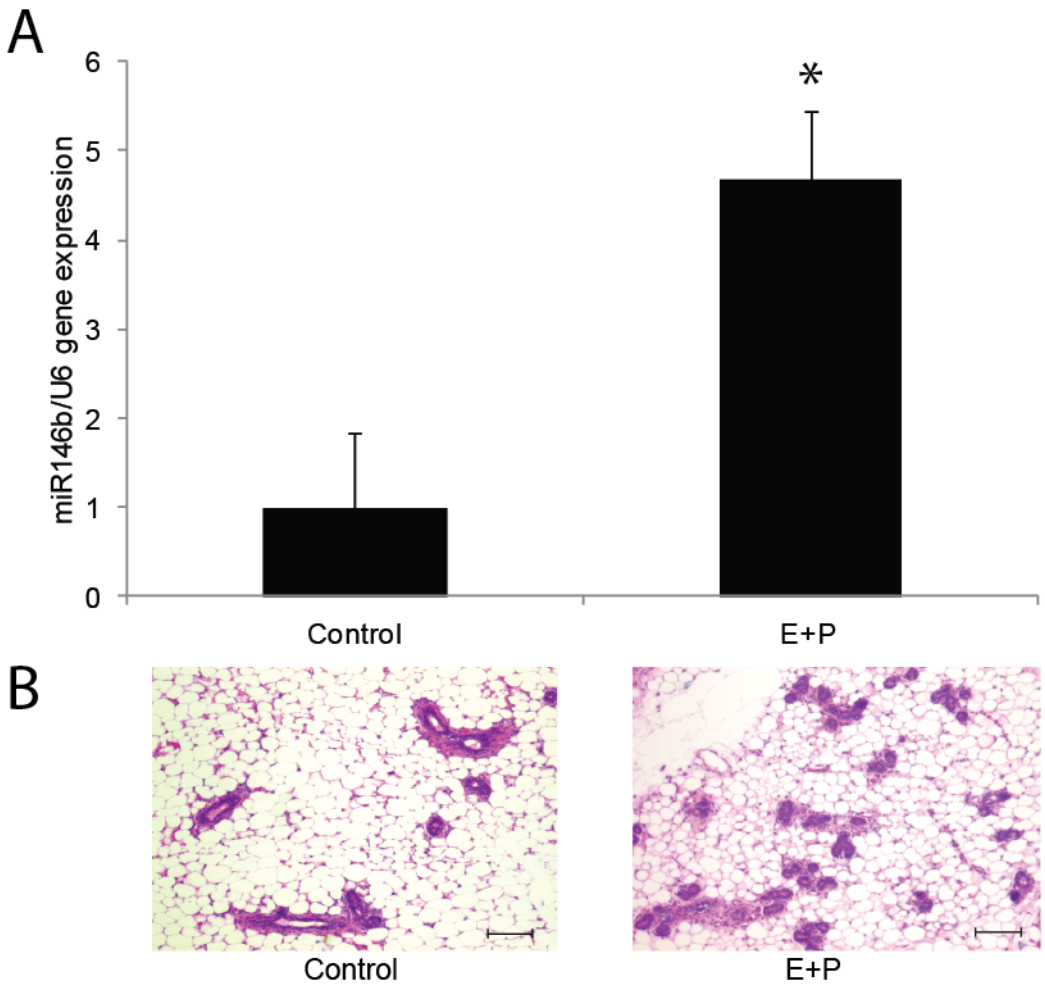

Figure 2. ***In vivo*** **administration of estrogen and progesterone results in upregulation of miR-146b expression in the mammary epithelial cells.** (*A*) Quantitative RT-PCR of miR-146b in PMEC from virgin mice treated with estrogen and progesterone for 3 weeks compared to non-treated virgin mice. Data is presented as the mean ± S.E.M. (n=4, * indicates $P<0.05$). (*B*) Representative H&E sections from the hormone treated and control mice.

MiR146b promotes survival of the alveolar progenitor cells

To assess the functional role of miR146b in the mammary alveolar progenitor cells, Locked Nucleic Acid oligonucleotides complementary to miR146b (LNA^{TM}, Exiqon) was used to knockdown and miR146b precursor transfection was used to overexpress miR146b in the pregnant primary epithelial cells derived from balb/C mammary glands and the CD derived alveolar progenitor cells. RT-qPCR was used to examine miR146a levels after knocking down miR146b in pregnant PMECs to check the specificity of the knockdown. The data showed a non-significant change in miR146a confirming that the knockdown is selective for miR146b (Fig. 3A). The cells were then collected at 72 hours post transfection, and stained with the LIVE/DEAD® Fixable Dead Cell Staining Kit. The fluorescent dye can permeate the compromised membranes of dead cells and react with free amines both in the interior and on the cell surface. Live-dead assay was performed on the distinct CD derived progenitor cells. MiR146b knockdown induced cell death selectively in the CD derived alveolar progenitor cells (Fig. 3B & C); and not in the ductal and the multipotent progenitor clones. Knockdown experiments showed no change in cell survival in the total population of PMECs derived from pregnant mouse mammary glands (data not shown). However, knockdown of miR146b reduced the percentage of the alveolar luminal progenitors ($lin^{-}CD29^{low}CD24^{high}CD61^{+}$) derived from pregnant mouse mammary glands by 45% (55%±9.7 SEM vs. 100%±1.8 SEM) compared to the controls (Fig. 3D & E) after maintaining the cells in culture for 3 days. Overexpression studies showed no significant increase in cell survival (data not shown).

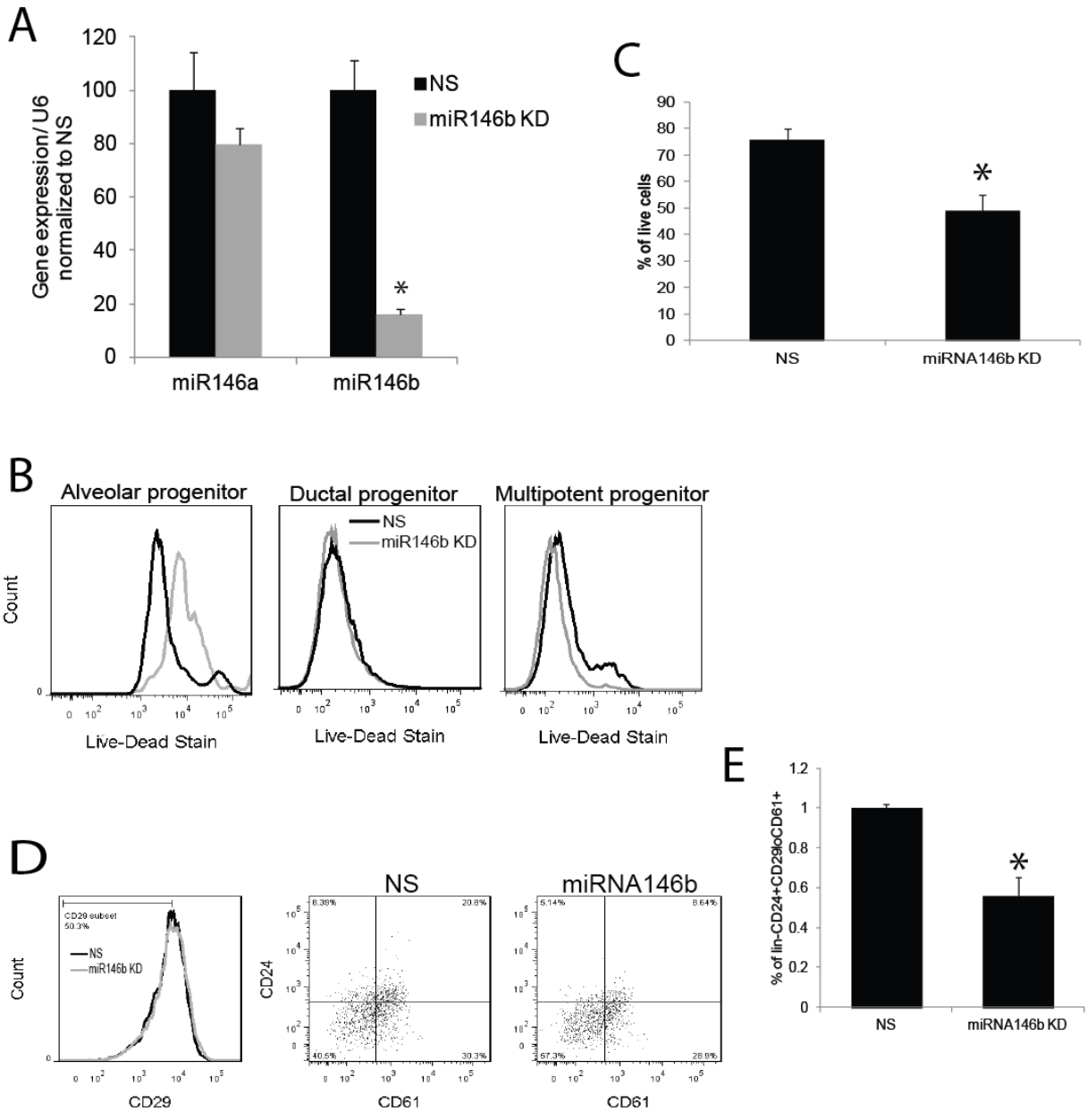
A
Gene expression/ U6 normalized to NS
120
100
80
60
40
20
0
NS
miR146b KD
*
miR146a
miR146b
C
% of live cells
90
80
70
60
50
40
30
20
10
0
*
NS
miRNA146b KD
B
Alveolar progenitor
Ductal progenitor
Multipotent progenitor
NS
miR146b KD
Count
Live-Dead Stain
Live-Dead Stain
Live-Dead Stain
E
% of lin-CD24+CD29loCD61+
1.2
1
0.8
0.6
0.4
0.2
0
*
NS
miRNA146b KD
D
CD29 subset
50.3%
NS
miR146b KD
Count
CD29
NS
miRNA146b
CD24
6.38%
20.8%
40.6%
30.3%
5.14%
8.64%
57.3%
28.9%
CD61
CD61

Figure 3. Knockdown of miR-146b leads to a reduction in the luminal progenitor subpopulation during pregnancy. (*A*) Quantitative RT-PCR of miR146a and miR146b in PMECs at 72 hours post-transfection with a miR146b LNA inhibitor (miR146b KD) and with non-silencing controls (NS; n=3, $P<0.05$). (*B*) Representative histogram of flow cytometry analysis for cells stained with the LIVE/DEAD® Fixable Dead Cell Staining Kit. Live-dead analysis was done in the alveolar progenitor cell line at 72 hours post-transfection, and (*C*) quantification of the percentage of live cells (n=3, $P<0.05$). (*D*) Representative flow cytometry dot plots of PMECs at 72 hours post-transfection analyzed for the $Lin^{-}CD24^{+}CD29^{lo}CD61^{+}$ population. (E) The reduction in the $CD24^{+}CD61^{+}$ progenitor population from the $Lin^{-}CD29^{lo}$ population of PMECs following knock down of miR-146b (n=3, * indicates $P<0.05$). Data is presented as the mean ±S.E.M.

MiR146b may promote alveolar progenitor cell maintenance by preferential regulation of STAT3β

We hypothesized that miR146b may promote alveolar progenitor cell survival during pregnancy and lactation by suppression of transcription factors with key roles during mammary development and or mammary involution process. Previous studies have shown miR146b targets to include IRAK1, TRAF6, NFkB, and SMAD4 [45,46]. Since some miRNAs might also up-regulate mRNA expression [47,48], STAT5a and Elf5 two transcription factors that promote alveologenesis, were also examined [49,50]. For these experiments, miR146b knock-down in the CD derived alveolar progenitor clone has been done to screen for the targets. As shown in Fig. 4A, knockdown of miR146b by LNA inhibitors did not up-regulate the expression of known targets of miR146b. These data suggest that the previously identified targets of miR146b are not regulated in the same manner in the mammary glands.

STAT3 is a transcription factor that has been previously implicated in promoting mammary epithelial cell apoptosis at the onset of gland involution [51]. This finding prompted us to examine whether miR146b might target STAT3. The 3' UTR of the STAT3 gene was analyzed with the RNA22 target prediction program [52], and two putative miR146b binding sites were indentified in the STAT3α 3'UTR (1.9 kb) (Fig. 5A). Knockdown of miR146b didn't change STAT3α levels in the CD derived alveolar progenitor clone, and increased up to 2-fold in pregnant PMECs (2.1 ± 1.04 SEM vs. 0.9 ± 0.04 SEM), while knockdown of miR146b increased STAT3β protein expression (Fig. 4B), up to 2-fold in the CD derived alveolar progenitor clone (3.0 ± 0.4 SEM vs. 1.3 ± 0.09 SEM; $p<0.05$), and up to 6-fold in pregnant PMECs compared to the controls (5.9 ± 1.7 SEM vs. 1.1 ± 0.07 SEM; $p<0.05$) . To correlate miR146b expression with STAT3α/β levels during mammary gland development, western blot of whole mammary glands

(undigested) from balb/c mice at different physiological stages of virgin, pregnant, lactating, and one, three, and six days post weaning were analyzed. Interestingly, STAT3β levels were inversely correlated to miR146b levels at each physiological stage, while STAT3α was equally expressed throughout all the stages (Fig. 4C). As shown previously [51] and in this study (Fig. 4D & E), there is an increase in STAT3α and STAT3β tyrosine phosphorylation (phosphor-Y705-STAT3, present in both STAT3α and STAT3β) prior to a significant rise in STAT3α serine phosphorylation (phosphor-S727-STAT3,present only in STAT3α) beginning at day 2 post-weaning. This suggests that STAT3β, either as homodimers or heterodimer with STAT3α or other transcription factors may contribute to the onset of mammary involution. The contribution of specific STAT3 isoforms to the process of mammary epithelial apoptosis at the onset of involution is not known at this time. The specific STAT3 isoform knockout mice have been generated but changes during mammary involution have not been evaluated [53].

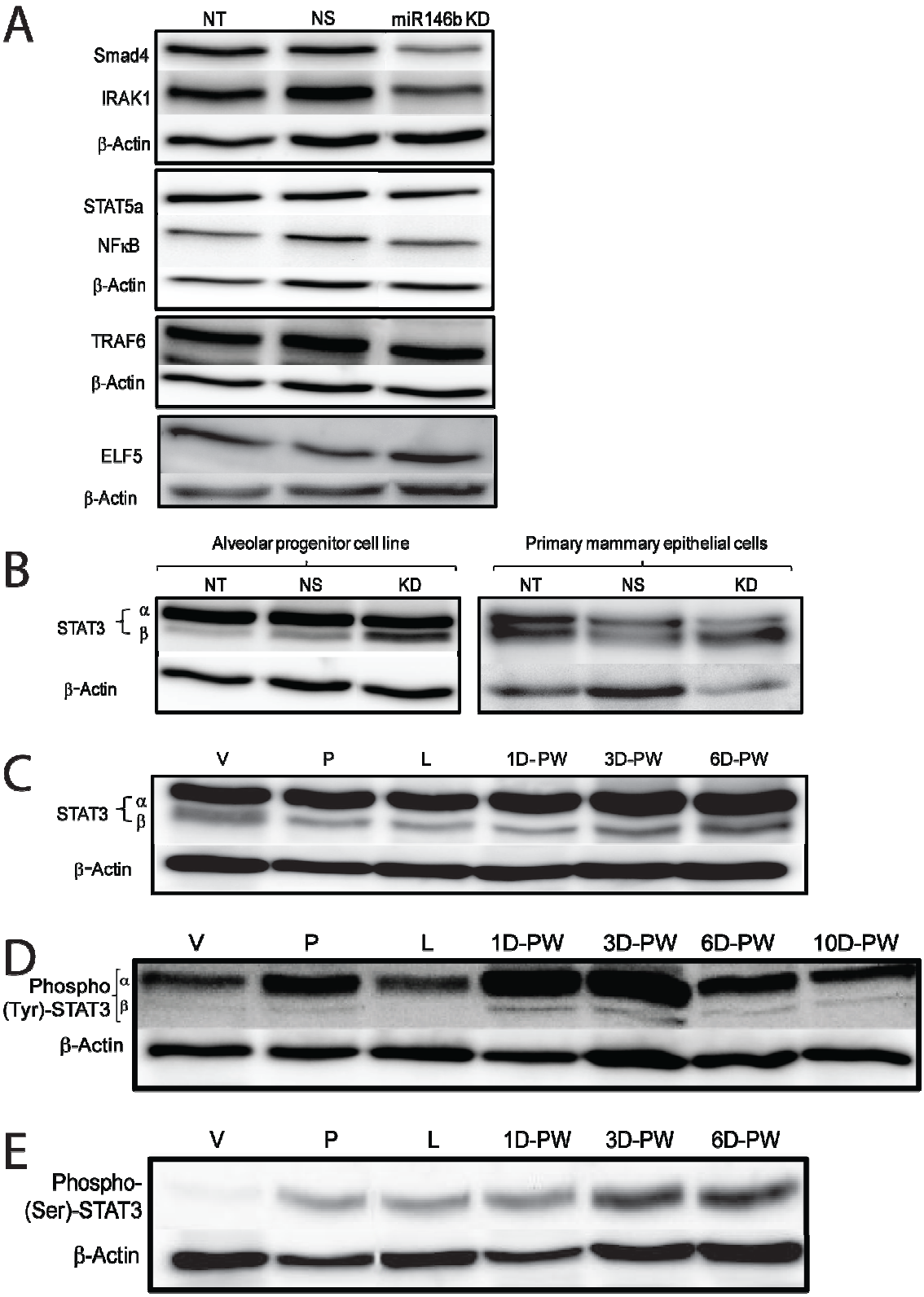
A
NT
NS
miR146b KD
Smad4
IRAK1
β-Actin
STAT5a
NFκB
β-Actin
TRAF6
β-Actin
ELF5
β-Actin
B
Alveolar progenitor cell line
Primary mammary epithelial cells
NT
NS
KD
NT
NS
KD
STAT3
α
β
β-Actin
C
V
P
L
1D-PW
3D-PW
6D-PW
STAT3
α
β
β-Actin
D
V
P
L
1D-PW
3D-PW
6D-PW
10D-PW
Phospho (Tyr)-STAT3
α
β
β-Actin
E
V
P
L
1D-PW
3D-PW
6D-PW
Phospho-(Ser)-STAT3
β-Actin

Figure 4. Effect of knockdown on miR146b known targets as well as on STAT3α/β. (*A*) Western analysis of Smad4, IRAK1, STAT5a, NFκB, TRAF6, ELF5, and β-Actin in the alveolar progenitor cell line 48 hours post-transfection in non-transfected (NT), NS, and miR146b KD cells. (*B*) Representative WB analysis of STAT3α/β levels in the alveolar progenitor clone (n=3) and in PMECs (n=4) at 48 hours post-transfection in NT, NS, and miR146b KD cells. (*C-E*) Western blot analysis of total STAT3α/β (*C*); Phosphorylated tyrosine 705 (Phospho-Tyr-STAT3) (*D*); Phosphorylated serine 727 (phosphor-ser-STAT3) (*E*) in total glands from mice at different physiological stages of virgin (V), pregnant (P), lactating (L), and involution days 1, 3, and 6 (*C, E*) and 10 (D) days post weaning (D-PW).

MiR146b binds to the 3'UTR of STAT3α

In order to determine if the putative miR146b binding sites within the 3' UTR of STAT3 gene, bind to miR146b, luciferase constructs where the 3'UTR of STAT3α was inserted downstream of the firefly luciferase reporter gene driven by SV40 promoter been utilized. A chimeric mRNA is transcribed consisting of the firefly luciferase and the STAT3α 3' UTR sequence. The vector also contains a renilla luciferase as an internal control downstream of the CMV promotor (Fig. 5B). In order to examine whether miR146b directly regulates STAT3α, 293T cells were transfected with the STAT3α 3'UTR reporter construct along with the miR146b precursor and the Pre-miR™ negative control. Firefly luciferase activity was then measured and normalized to renilla luciferase activities in the same wells. The results showed a statistically significant reduction ($P<0.0001$) in luciferase reporter activity when cells overexpressed miR146b compared with cells that expressed the Pre-miR™ negative control (Fig. 5C). Luciferase reporter activity of the STAT3α3'UTR was also significantly lower in PMECs from pregnant mice, when miR146b expression is significantly higher, compared to luciferase activity in PMEC from virgin mice ($P<0.0001$; Fig. 5D). These data suggest that miR146b directly binds the 3'UTR of STAT3α, and it is unclear how miR146b binds STAT3α 3'UTR without significantly affecting STAT3α protein levels. STAT3β may have a longer half-life resulting in a more stable protein compared to STAT3α. A more stable/longer acting miRNA146b knock down strategy will need to be used in order to examine this possibility. Furthermore, it is still possible that miR146b binding is playing a role in STAT3 alternative splicing events, and these possibilities are being explored. Real-time RT–PCR results (data not shown) confirmed that STAT3α and STAT3β mRNA levels in miR146b knockdown cells at 48 hours after transfection remain

constant despite striking changes in protein expression. This finding rules out the affect of miR146b on splicing. However, site directed mutagenesis will be done to further validate these miR146b seed sites in the 3'UTR. The computationally predicted target sites in the miRNA-binding seed regions will be mutated in order to examine the role of direct binding of miR146b to the 3'UTR of STAT3.

There are conflicting reports about the STAT3β 3'UTR sequence. Ensemble [54] reports STAT3β 3'UTR length as 3.6 kb which is 1.7 kb longer than STAT3α, and has three putative miR146b binding sites. Several attempts to clone this sequence have failed. On the other hand, NCBI [55] reports that the STAT3β 3'UTR to be 2 kb, which is identical to the STAT3α 3'UTR with extra 90 base pairs in the 5' end. This includes the same two putative binding sites as STAT3α. In this case, preferential STAT3β suppression may be because of the slightly longer 3'UTR in STAT3β which may change the 3'UTR secondary structure in a way to make it more accessible for miR146b binding. Regulation of splicing events may also be another possible mechanism by which miR146b affects differential expression of STAT3β. We are in the process of cloning STAT3β 3'UTR luciferase reporter construct and examining its suppression by miR146b.

Our results suggest that miR146b upregulation during lactation and pregnancy function to suppress STAT3β expression thus maintaining the survival of mammary alveolar progenitor cells. Down regulation of miR146b during involution may result in removal of STAT3β suppression followed by alveolar progenitor cell death and involution.

A

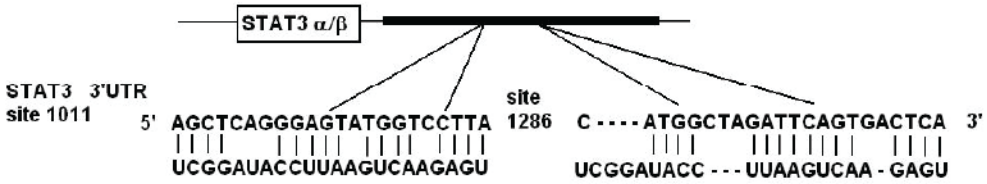
STAT3 α/β
STAT3 3'UTR
site 1011
5' AGCTCAGGGAGTATGGTCCTTA
UCGGAUACCUUAAGUCAAGAGU
site
1286
C - - - - ATGGCTAGATTCAGTGACTCA 3'
UCGGAUACC - - - UUAAGUCAA - GAGU

B

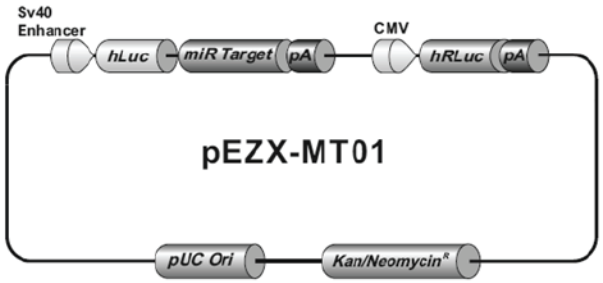
Sv40
Enhancer
hLuc
miR Target
pA
CMV
hRLuc
pA
pEZX-MT01
pUC Ori
Kan/Neomycin^R

C

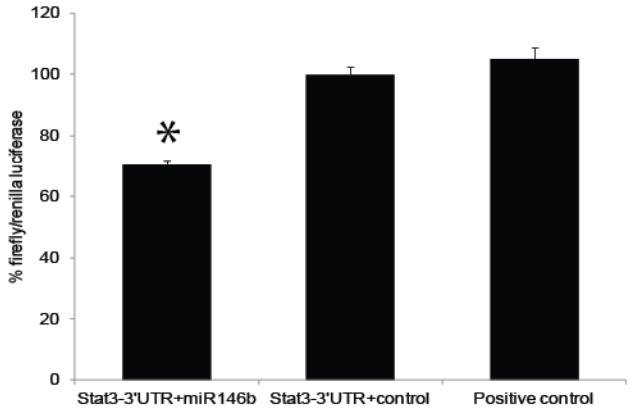
120
100
80
60
40
20
0
% firefly/renilla luciferase
*
Stat3-3'UTR+miR146b
Stat3-3'UTR+control
Positive control

D

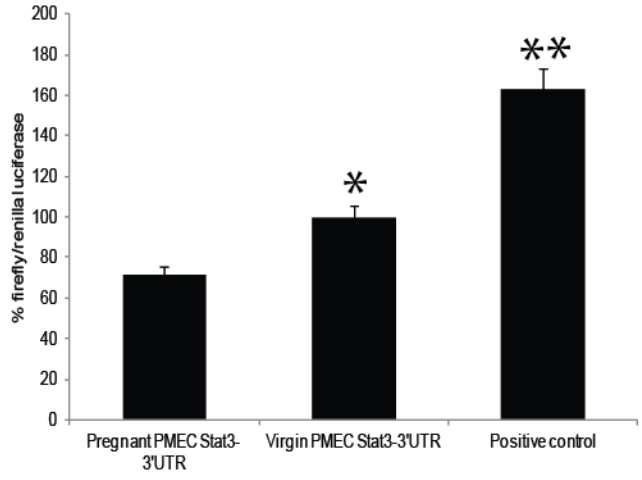
200
180
160
140
120
100
80
60
40
20
0
% firefly/renilla luciferase
*
**
Pregnant PMEC Stat3-3'UTR
Virgin PMEC Stat3-3'UTR
Positive control

Figure 5. MiR-146b targets the 3'UTR of STAT3α/β. (*A*) An illustration of the 3'UTR of STAT3α/β computationally predicted binding sites for miR-146b. (*B*) Vector backbone of STAT3α/β 3' UTR reporter construct, STAT3α/β 3'UTR sequence was inserted downstream of the firefly luciferase reporter gene, driven by SV40 promoter for expression, renilla luciferase was used as an internal control. (*C*) Luciferase reporter activity of the STAT3α/β 3′UTR in 293T cells expressing miR146b, the non-silencing hairpin negative control and the luciferase positive control. Reporter activity decreases by 30% when cells are overexpressing miR146b. Each sample was normalized to Renilla luciferase activity. (n=6,*$P<0.0001$). (*D*) Luciferase reporter activity of the STAT3α/β 3'UTR in PMECs from pregnant and virgin mice without treatment, and in PMEC treated with the luciferase positive control. (n=6,*$P<0.0001$)

Discussion

In this study we demonstrate that miR146b expression is highly upregulated in the alveolar progenitor cells, during pregnancy and lactation and with hormonal (E plus P) stimulation. The transient knockdown of this miRNA affects the survival of luminal alveolar progenitor cells. This suggests that miR146b might be upregulated during the process of alveologenesis under the influence of hormones, causing suppression of key transcription factors involved in the process of involution and alveolar cell death

Using flow analysis and cell sorting of mouse mammary epithelial cells, we showed miR146b to be highly expressed in the luminal progenitor subpopulation of cells. Bockmeyer et al. studied the miRNA profiles of healthy human basal and luminal epithelial cells as well as basal and luminal breast cancers. The luminal and basal epithelial cells were isolated by laser assisted microdissection from immunohistochemically stained tissue sections of healthy human breast specimens. Interestingly, miR146b was shown to be a basal-specific miRNA and to be expressed at higher levels in basal-like breast cancers compared to luminal A and B subtypes [39]. Other than this report, expression of miR146b and its role in mammary epithelial cell development has not been previously described.

Knock-down of miR146b in the luminal progenitor cells reduced cell survival. We reasoned that miR146b might play a role in alveolar cell maintenance by regulating a known target such as IRAK1/TRAF6, NF-κB, or SMAD4 and or by regulating transcription factors with known roles during alveologenesis such as STAT5α and ELF5. A review of the literature showed miR146b to regulate TGF-β signaling by repressing SMAD4 in thyroid cancers [46]. TGF-β has been shown to play an important role during mammary involution by inducing cellular apoptosis and alveolar collapse in the early stages of involution [56]. Furthermore, miR146b has been shown

to inhibit breast cancer cell invasion and migration by targeting IRAK1/TRAF6 and by down regulation of NF-kB signaling [45]. NF-kB has also been shown to destabilize STAT5α, a key transcription factor that promotes alveologenesis [57]. Interestingly, miR146b knockdown did not result in the up-regulation of any of these suspected targets. Therefore, the previously identified miR146b targets may not be similarly regulated in the mammary glands.

Since STAT3 transcription factors were reported to play key roles in mammary epithelial cell apoptosis at the onset of involution, we explored the role of miR146b in regulating STAT3 isoforms. STAT3 has two main isoforms: the full-length STAT3α and the truncated STAT3β, by alternative mRNA splicing of exon 23 [15,16]. In STAT3β, the 55-amino acid C-terminal acidic transactivation domain of STAT3α is replaced by seven unique amino acid residues [16]. An important factor in STAT3 functional heterogeneity may be the existence of these two alternatively spliced isoforms. As suspected, miR146b knockdown resulted in up-regulation of STAT3 expression in both PMEC derived from pregnant mammary glands and in the alveolar progenitor cells. However, the up-regulation of STAT3β isoform was higher than that of STAT3α. There are several possibilities for preferential regulation of STAT3b protein expression by MiR146b. One is the existence of an additional miR146b binding site on the predicted STAT3b 3'UTR resulting in higher suppression of STAT3b protein translation [54]. Another key mechanism, may be the regulation of alternative splicing events. The interplay between the miRNA and splicing regulation has been previously demonstrated. These studies showed that miR124 and miR133 regulate the RNA-binding protein, polypyrimidine tract-binding protein 1 (PTBP1). PTBP1 is a global repressor of alternative pre-mRNA splicing in non neuronal cells [60,61]. Additionally, ESEfinder and PESX algorithms predicted a putative exonic splicing enhancer (ESE), which overlaps with one of the predicted miR146b binding

sites. MiR146b binding to this overlapped region may regulate ESE. MiR146b could also indirectly regulate STAT3 alternative splicing by targeting key splicing factors. Real-time RT–PCR results showed that STAT3α and STAT3β mRNA levels remain constant in miR146b knockdown cells despite striking changes in protein expression suggesting that miR146b most likely affects STAT3 protein translation.

STAT3 is characterized by its capacity to activate different sets of genes in different cell types [62], and the different STAT3 isoforms seem to regulate cell survival and maintenance in a cell type and context specific manner by suppression and or activation of a variety of target genes [19]. STAT3β has been considered a dominant-negative factor by inhibiting STAT3α gene transactivation [17,18]. More recent studies have demonstrated that STAT3β may activate a specific set of genes and possess non-redundant functions to STAT3α. Zammarchi et. al used morpholino oligomers to redirect endogenous STAT3 alternative splicing from STAT3α to STAT3β. This study showed that the induction of the STAT3β isoform in MDA-MB-435 cells caused cell death and tumor regression in the xenograft models. The same study showed that STAT3 canonical target genes were not affected by the switch from STAT3α to STAT3β. Rather, a unique expression signature seems to be associated with the physiological α-to-β splicing shift [16]. In mammary gland development, it has become clear that STAT3 regulates a complex series of processes involving alveolar epithelial cell death during involution by maintaining the balance of inflammatory and anti-inflammatory signaling [19]. The contribution of specific STAT3 isoforms to mammary involution process is still not known. Mice knockout of specific STAT3 isoforms have been generated [53]. It is reported that STAT3β knockout mice are viable and fertile and capable of nursing their pups [53]. However, a detailed characterization of the mammary glands during involution has not been reported in these mice.

Our study clearly demonstrates that both isoforms of STAT3 are up-regulated during involution. It would be interesting to decipher the contribution of specific STAT3 isoforms to the mammary involution process.

Our study is the first to demonstrate that sex hormones regulate the expression levels of miR146b. Furthermore, miR146b levels rise during mammary lactation and pregnancy. MiR146b up-regulation during pregnancy and lactation may mediate the maintenance of alveolar progenitor cells by selective suppression of STAT3β and to a lesser extent STAT3α. Following weaning and during the process of involution miR146b levels drop to basal levels which may result in the up-regulation of STAT3 isoforms and induction of alveolar cell death (Fig. 6; Model). The LNA inhibitors induce a transient knockdown in miR146b [63], thus they are not suitable for long term *in vivo* transplantation studies. It will be interesting to explore the effect of miR146b on alveologenesis by using a more stable knockdown and overexpression approach following in vivo transplantation. The increasing reports demonstrating the role of miR146a/b in various types of human cancers, and our finding that miR146b may regulate the expression of STAT3 isoforms, known transcription factors that mediates both the process of involution and breast cancer, may shed light to the current understanding of cellular pathways leading to malignant transformation in the mammary epithelium.

Chapter III: Materials and Methods

Cell lines

CommaDβ derived clones (SP-1, SP-3, SP-4, NSP-1, NSP-2, NSP-3, NSP-4, and NSP-5) were used. The alveolar progenitor (SP-3), ductal progenitor (NSP-2) and multipotent progenitor clones (NSP-5) have been previously described and characterized [2]. 293T cells (Clontech, Cat# 632180) were used for luciferase reporter assays.

Animals

We used female balb/c mice which were either bred or purchased from Harlan Laboratories, Inc., IN, USA. We used mice in late pregnancy, as well as mice 24 hours, 3 days, and 6 days post weaning (involuting mammary glands), and virgin mice in the metestrous phase of the estrous cycle as confirmed by vaginal cytology [64]. Animal experiments were conducted following protocols approved by the University of Kansas Medical Center Institutional Animal Care and Use Committee.

Mouse surgeries

Slow-releasing pellets containing 50 μg of estradiol and 20 mg of progesterone for hormonal treatment were placed subcutaneously on the lateral side of the neck between the ear and shoulder. After 3 weeks, mice were sacrificed, and the mammary glands were excised. One mammary gland was processed for embedding, and the other mammary gland was used to recover the epithelial cells according to established protocol in our laboratory [65].

Cell culture: 2D/ 3D (Matrigel^{TM})

Primary mouse cells were grown and maintained in F12 (Invitrogen, Cat# 11765) supplemented with 5% fetal Bovine serum (Invitrogen, Cat# 10438026), 1% antibiotic/antimycotic reagents (AA; Invitrogen, Cat# 15240), 50μg/ml gentamicin (Sigma-Aldrich Cat# G1272), 1mg/ml hydrocortisone (Stem Cell Technologies, Cat# 07904), and 5 ng/ml epidermal growth factor. The CD derived clones (i.e. SP-3, NSP-2 and NSP-5) were grown in DMEM/F12 (Invitrogen, Cat# 11320) containing 2% fetal bovine serum, 5 ng/ml epidermal growth factor, 10 mM HEPES (Invitrogen, Cat#15630), 5μg/ml insulin, 50μg/ml gentamicin, and 1% antibiotic/antimycotic.

293T cells were grown in DMEM (Sigma-Aldrich, Cat# D5796) containing 10% fetal bovine serum, and 1% antibiotic/antimycotic. The cells were grown in humidified incubator at 37^{o}C and 5% CO_2. For 3D culture, cells were plated in media containing 2% BD Basement Membrane Matrix Matrigel^{TM} (BD Biosciences, Cat# 356234) on a thin film of, Matrigel^{TM}. Cell recovery was achieved using BD Cell Recovery Solution (BD Biosciences, Cat# 354253).

Hematoxylin and eosin staining

Excised mammary glands were fixed in 4% paraformaldehyde for 2 hours on ice followed by 70% ethanol at 4^{o}C until processing. Tissues were embedded in paraffin and stained for hematoxylin and eosin according to established protocols [65].

RNA Isolation and Quantitative PCR (qPCR):

Total RNA was isolated with miRNeasy Mini Kit (Qiagen Cat# 217004) using the manufacturer's protocol, and cDNA was synthesized from 250 ng of total RNA with miScript Reverse Transcription Kit (Qiagen Cat# 218061). MiRNA and mRNA were measured using

miScript SYBR Green PCR Kit (Qiagen, Cat# 218073), and primers specific for hsa-miR-146b-5p (IDT, Ref# 52053397). Reactions were performed in the StepOnePlus™ Real-Time PCR System and software (Applied Biosystems) in 96-well plates at 95^{o}C for 15min, followed by 40 cycles of 94^{o}C for 15 s, 55^{o}C for 30 s and 70^{o}C for 30 s. Target gene expression was normalized to snU6: snU6 forward (IDT Ref.# 50315659), snU6 reverse (IDT Ref# 50315660). The standard curve method was used for quantification.

Microarray studies

RNA from CDβ clones with growth potential (SP-3, NSP-1, NSP-2, NSP-5) and those without growth potential (NSP-3, NSP-4, SP-1, SP-4) were combined. RNA quantity and quality (RIN>8) was checked using the Agilent Bioanalyzer. Reverse transcription was done using SA Biosciences RT^2 miRNA First Strand Kit, RT^2 miRNA PCR Array System (human cancer array, SABiosciences MAH-102E). PCR array was loaded according to SA Biosciences protocol for loading map. The data was analyzed using the ΔΔCT method. (www.sabiosciences.com/pcrarraydataanalysis.php).

FACS analysis and sorting

Primary antibodies used were anti-mouse CD29 (APC/Cy7)-conjugated antibody (Biolegend, Cat# 102226), anti-mouse CD24 (PE)-conjugated antibody (BD Biosciences, Cat# 553262), anti-mouse CD61 (Alexa Fluor 647)-conjugated (Biolegend, Cat# 104314), biotin-conjugated anti-mouse CD31 (Biolegend, Cat# 102404), biotin-conjugated anti-mouse CD140a (Biolegend, Cat# 135910), biotin-conjugated Rat anti-mouse CD45 (BD Pharmingen, Cat# 553077), biotin-conjugated Rat anti-mouse Ter-119 (BD Pharmingen, Cat# 559971). The biotin-conjugated

antibodies were labeled using Streptavidin-V450 (BD Biosciences, Cat# 560797). Isotype control staining was performed using PE-conjugated anti-rat immunoglobulin G2bk (IgG2bk) antibody (Biolegend, Cat# 400635), APC/Cy7-conjugated mouse IgG2bk antibody (BD Pharmingen, Cat# 558061) and biotin-conjugated rat IgG2ak (IgG2ak) antibody (BD Pharmingen, Cat# 553928). The cells were stained at a final concentration of 1:200 for 30 minutes on ice followed by washes in Hanks' balanced salt solution (Invitrogen, Carlsbad, CA, USA) containing 2% fetal bovine serum. For live dead assay LIVE/DEAD® Fixable Dead Cell Stain Kit (Invitrogen, Cat# L34955) was used per manufacturer's protocol. FACS and data analysis were performed using the BD LSR II flow cytometer and FlowJo software (Tree Star, Inc., Ashland, OR, USA). Cell sorting was performed using the FACS Aria (BD Biosciences, San Jose, California, USA).

MiR146b knock down and over expression in CDβ clones and in PMEC

To overexpress miR-146b, 40nM of hsa-miR-146b-5p synthetic pre-miR precursors (Ambion, Ref# AM17100) were transfected into PMEC, along with the Pre-miR^{TM}miRNA Precursor Negative Control #1 (Ambion Ref# AM17110). To knockdown miR-146b, 40 nM of miRCURY LNA microRNA inhibitor (Exiqon, Cat# 410066-04) for hsa-miR-146b-5pwas transfected into the cell lines and PMEC.

Because the human and murine miR-146b-5p have identical sequences, the use of products, pre-miRs and LNA inhibitors, designed for human are a perfect match for the mouse. MiRCURY LNA microRNA inhibitor control (Exiqon, Cat#199004-04) was used as a negative control. In both cases, cells were seeded in a six-well plate and transfected 24h later with Lipofectamine^{TM} 2000 Transfection Reagent (Invitrogen, Cat# 11668-019) in the media described above, without

serum or antibiotic present. 24h after transfection the cells were nourished with 1% serum. Seventy-two hours post-transfection, the cells were washed with PBS and recovered for analysis as described above.

Ugagaacugaauuccauggguu 146a

Ugagaacugaauuccauaggcu 146b

Western blot

Cells were lysed on ice using RIPA buffer (50 mM Tris-HCL, pH 7.4, 150 mM NaCl, 2 mM EGTA, 0.25% deoxycholate and 1% Triton X-100) containing protease inhibitors (Calbiochem, Cat# 535140) and phosphatase inhibitors (Calbiochem, Cat# 524627). The protein extracts were prepared by collecting supernatants after centrifugation at 12,000 xg at 4^{o}C for 30 min. The protein concentrations were measured using BCA protein assay kit according to manufacturer's protocol (Thermo Scientific, Cat# 23250). Ten μg of protein was separated on an 8-10% SDS-PAGE gel, transferred onto PVDF membrane (Millipore, 0.45 mm) in Tris-Glycine (25 mM tris and 192 mM glycine, pH 8.3, BioRad, Cat# 161-0771) containing 20% v/v methanol at 100V for 2 hours. The PVDF membrane was blocked with 5% non-fat dry milk in TBS containing 0.05% Tween 20 (TBST) at room temperature for 1 hour. The blots were washed three times for 10 min with TBST before incubating with primary antibody in TBST for 1 hour at room temperature or overnight at 4^{o}C. The primary antibodies STAT5a (Invitrogen, Cat# 13-3600), STAT3 (K-15; Santa Cruz, Cat# sc-483), p(Ser)-STAT3 (23G5; Santa Cruz, Cat# sc-56747), p(Tyr)-STAT3 (Cell signaling, Cat# 9131S) TRAF6 (H-274; Santa Cruz, Cat# sc-7221), IRAK1 (H-273; Santa Cruz, Cat# sc-7883), STAT5a (ST5a-2H2; Invitrogen, Cat# 13-3600), NFkB p65

(C22B4;Cell Signaling, Cat# 4764), ELF5 (N-20; Santa Cruz, Cat# sc-9645), and Smad4 (B-8; Santa Cruz, Cat# sc-7966) were used at a dilution of 1:1000. Following primary antibody incubation, the membranes were washed thoroughly with TBST (3x, 10 min each) and incubated with horseradish peroxidase (HRP) conjugated secondary antibodies Donkey anti-rabbit-HRP (Jackson, Cat# 711-035-152) at 1:10,000 or goat anti-mouse-HRP (Santa Cruz, Cat# sc2005) at 1:10,000 in TBST containing 1% milk for 1 hour at room temperature. After washing with TBST (3x, 10 min each), the bands were visualized with enhanced chemiluminescence (ECL) , SuperSignal West Femto Kit (Thermo Scientific, Cat# 34095) and the blots were digitalized using Auto Chemi systems (UVP Inc., Upland, CA). The membranes were stripped by incubating with stripping buffer (50 mM Tris-HCL, pH 6.8, 2% SDS, and 100 mM β-marcaptoethanol) at 50^{o}C for 30 min followed by washing with TBST and re-probed with β-actin antibody (Santa Cruz, Cat# sc1616, 1:1500 dilution) followed by anti-goat IgG HRP (Santa Cruz, Cat# sc2350, 1:10000 dilution) for loading control. Densitometry analysis was performed using LabWorks software (UVP Inc., Upland, CA).

Luciferase Reporter Constructs

293T cells (Clontech, Cat# 632180) were plated in 6-well plates. After 24h, the cells were transfected with 1.0 µg of STAT3α 3' UTR miRNA target sequence expression clone in pEZX-MT01 vector with fLuc (Genecopoiea, Cat# MmiT043695) and 40nM of miR-146b precursor miRNA (Ambion, Ref# AM17100) and miRNA control (Ambion Ref# AM17110). The cells were transferred to a 96-well plate 18 hours after transfection and cultured for another 24 hours. Both firefly luciferase and renilla luciferase activities were measured using GeneCopoeia Luc-Pair™ miR Luciferase Assay kit (Genecopoiea, Cat# LPFR-M030) according to the

manufacturer's protocol and data was recorded on BioTek Microplate Reader using Gen5^{TM}software. Firefly luciferase activity was normalized with renilla luciferase activities in the same well.

Chapter IV: Conclusion

In conclusion, our study is the first to demonstrate that miR146b is a hormonally regulated miRNA, which is up-regulated during pregnancy and lactation, and its expression is higher in the luminal progenitor subpopulation of cells. MiR146b might not only be involved in normal cell function, but its mis-regulation might contribute to cancer initiation, progression and metastasis. We showed that miR146b knockdown reduces the luminal progenitor cells, which might be important in the etiology of cancer. Furthermore, we demonstrated that miR146b can regulate the expression of different STAT3 isoforms, especially STAT3β. The role of STAT3 in mammary gland involution has been widely accepted, but the individual role of STAT3 isoforms is still unclear. Generation of loss-of-function mouse models for miR146b will be required to establish whether miR146b is essential for normal development, and the functional role of STAT3β in mammary gland involution requires further investigation. Finally, our results led us to a proposed mechanism by which miR146b my play a role in alveologenesis and mammary gland remodeling. In this model, miR146b up-regulation during pregnancy and lactation may mediate the maintenance of alveolar progenitor cells by selective suppression of STAT3β and to a lesser extent STAT3α. Following weaning and during the process of involution miR146b levels drop to basal levels which may result in the up-regulation of STAT3 isoforms and induction of alveolar cell death (Fig. 6; Model).

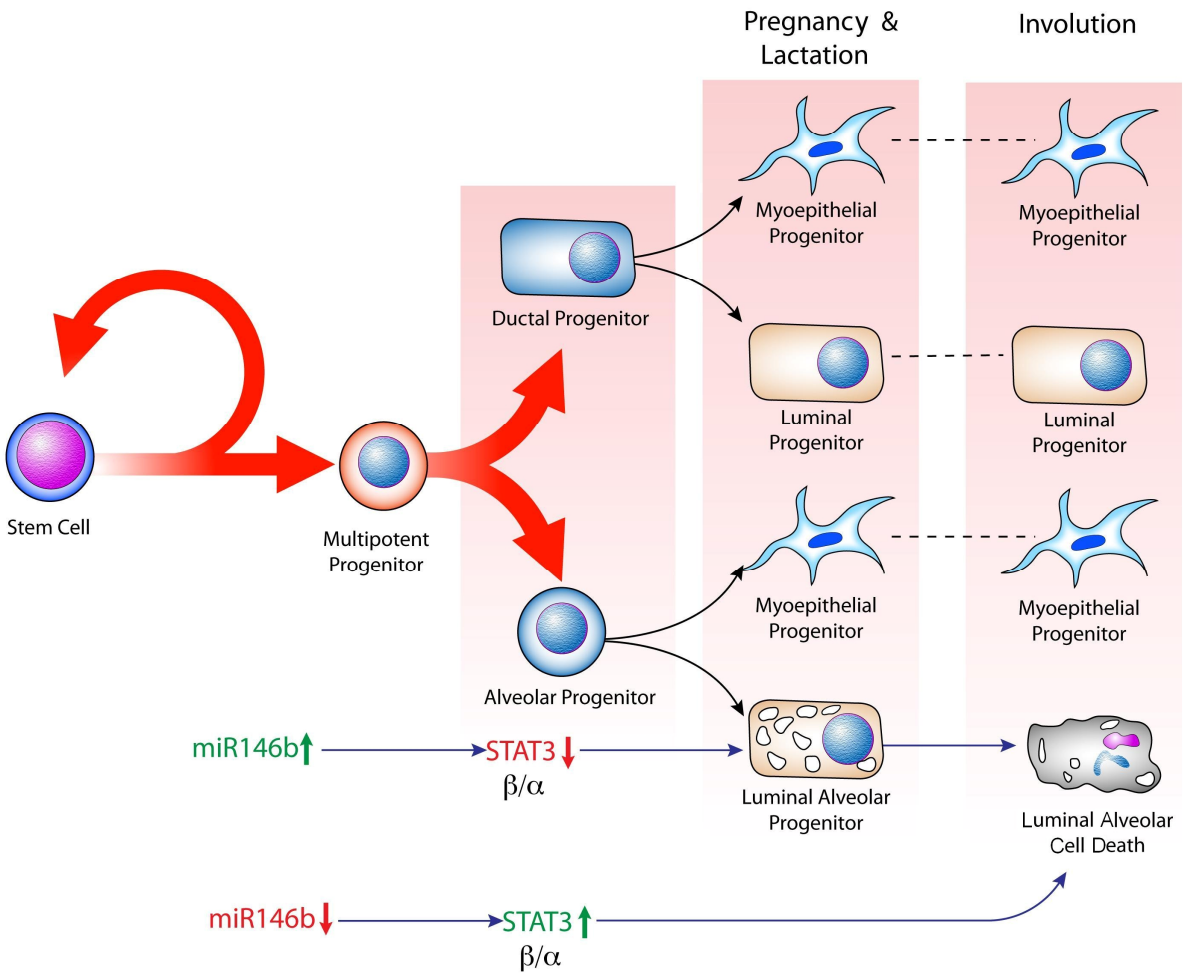
Pregnancy &
Lactation
Involution
Myoepithelial
Progenitor
Myoepithelial
Progenitor
Ductal Progenitor
Luminal
Progenitor
Luminal
Progenitor
Stem Cell
Multipotent
Progenitor
Myoepithelial
Progenitor
Myoepithelial
Progenitor
Alveolar Progenitor
miR146b
STAT3
β/α
Luminal Alveolar
Progenitor
Luminal Alveolar
Cell Death
miR146b
STAT3
β/α

Figure 6. A proposed model for miR-146b regulation of alveolar progenitor cell maintenance. Mammary epithelial cell hierarchy begins with asymmetric self-renewal in the stem cells, which generate multipotent and bipotent ductal and alveolar progenitor cells. Ductal and alveolar progenitor cells give rise to luminal and myoepithelium-restricted progenitors. During pregnancy and lactation, miR146b may be upregulated under the influence of estrogen and progesterone in the alveolar progenitor cells to suppress STAT3α/β and to promote the survival of these cells. During involution, miR-146b may be down regulated in the alveolar progenitors to de-represses STAT3α/β followed by cell death in the luminal alveolar cells and the onset of involution.

Chapter V: References

1. Visvader JE (2009) Keeping abreast of the mammary epithelial hierarchy and breast tumorigenesis. Genes Dev 23: 2563-2577.

2. Kittrell FS, Carletti MZ, Kerbawy S, Heestand J, Xian W, et al. (2011) Prospective isolation and characterization of committed and multipotent progenitors from immortalized mouse mammary epithelial cells with morphogenic potential. Breast Cancer Res 13: R41.

3. Shackleton M, Vaillant F, Simpson KJ, Stingl J, Smyth GK, et al. (2006) Generation of a functional mammary gland from a single stem cell. Nature 439: 84-88.

4. Stingl J, Eirew P, Ricketson I, Shackleton M, Vaillant F, et al. (2006) Purification and unique properties of mammary epithelial stem cells. Nature 439: 993-997.

5. Asselin-Labat ML, Sutherland KD, Barker H, Thomas R, Shackleton M, et al. (2007) Gata-3 is an essential regulator of mammary-gland morphogenesis and luminal-cell differentiation. Nat Cell Biol 9: 201-209.

6. Regan JL, Kendrick H, Magnay FA, Vafaizadeh V, Groner B, et al. (2012) c-Kit is required for growth and survival of the cells of origin of Brca1-mutation-associated breast cancer. Oncogene 31: 869-883.

7. Smalley MJ, Clarke RB (2005) The mammary gland "side population": a putative stem/progenitor cell marker? J Mammary Gland Biol Neoplasia 10: 37-47.

8. Watson CJ, Khaled WT (2008) Mammary development in the embryo and adult: a journey of morphogenesis and commitment. Development 135: 995-1003.

9. Wagner KU, Boulanger CA, Henry MD, Sgagias M, Hennighausen L, et al. (2002) An adjunct mammary epithelial cell population in parous females: its role in functional adaptation and tissue renewal. Development 129: 1377-1386.

10. Nandi S (1958) Endocrine control of mammarygland development and function in the C3H/ He Crgl mouse. J Natl Cancer Inst 21: 1039-1063.

11. Lyons WR (1958) Hormonal synergism in mammary growth. Proc R Soc Lond B Biol Sci 149: 303-325.

12. Imagawa W, Pedchenko VK, Helber J, Zhang H (2002) Hormone/growth factor interactions mediating epithelial/stromal communication in mammary gland development and carcinogenesis. J Steroid Biochem Mol Biol 80: 213-230.

13. Manni A, editor (1999) Endocrinology of breast cancer. Totawa, New Jersey 07512: Humana Press Inc. 391 p.

14. Hennighausen L, Robinson GW (2001) Signaling pathways in mammary gland development. Dev Cell 1: 467-475.

15. Huang Y, Qiu J, Dong S, Redell MS, Poli V, et al. (2007) Stat3 isoforms, alpha and beta, demonstrate distinct intracellular dynamics with prolonged nuclear retention of Stat3beta mapping to its unique C-terminal end. J Biol Chem 282: 34958-34967.

16. Zammarchi F, de Stanchina E, Bournazou E, Supakorndej T, Martires K, et al. (2011) Antitumorigenic potential of STAT3 alternative splicing modulation. Proc Natl Acad Sci U S A 108: 17779-17784.

17. Caldenhoven E, van Dijk TB, Solari R, Armstrong J, Raaijmakers JA, et al. (1996) STAT3beta, a splice variant of transcription factor STAT3, is a dominant negative regulator of transcription. J Biol Chem 271: 13221-13227.

18. Schaefer TS, Sanders LK, Nathans D (1995) Cooperative transcriptional activity of Jun and Stat3 beta, a short form of Stat3. Proc Natl Acad Sci U S A 92: 9097-9101.

19. Pensa S, Watson CJ, Poli V (2009) Stat3 and the inflammation/acute phase response in involution and breast cancer. J Mammary Gland Biol Neoplasia 14: 121-129.

20. Hughes K, Wickenden JA, Allen JE, Watson CJ (2011) Conditional deletion of Stat3 in mammary epithelium impairs the acute phase response and modulates immune cell numbers during post-lactational regression. J Pathol.

21. Burke WM, Jin X, Lin HJ, Huang M, Liu R, et al. (2001) Inhibition of constitutively active Stat3 suppresses growth of human ovarian and breast cancer cells. Oncogene 20: 7925-7934.

22. Huang M, Page C, Reynolds RK, Lin J (2000) Constitutive activation of stat 3 oncogene product in human ovarian carcinoma cells. Gynecol Oncol 79: 67-73.

23. Watson CJ, Miller WR (1995) Elevated levels of members of the STAT family of transcription factors in breast carcinoma nuclear extracts. Br J Cancer 71: 840-844.

24. Garcia R, Yu CL, Hudnall A, Catlett R, Nelson KL, et al. (1997) Constitutive activation of Stat3 in fibroblasts transformed by diverse oncoproteins and in breast carcinoma cells. Cell Growth Differ 8: 1267-1276.

25. Wagner KU, Schmidt JW (2011) The two faces of Janus kinases and their respective STATs in mammary gland development and cancer. J Carcinog 10: 32.

26. Greene SB, Herschkowitz JI, Rosen JM (2010) Small players with big roles: microRNAs as targets to inhibit breast cancer progression. Curr Drug Targets 11: 1059-1073.

27. He L, Hannon GJ (2004) MicroRNAs: small RNAs with a big role in gene regulation. Nat Rev Genet 5: 522-531.

28. Kanellopoulou C, Muljo SA, Kung AL, Ganesan S, Drapkin R, et al. (2005) Dicer-deficient mouse embryonic stem cells are defective in differentiation and centromeric silencing. Genes Dev 19: 489-501.

29. Andl T, Murchison EP, Liu F, Zhang Y, Yunta-Gonzalez M, et al. (2006) The miRNA-processing enzyme dicer is essential for the morphogenesis and maintenance of hair follicles. Curr Biol 16: 1041-1049.

30. Bernstein E, Kim SY, Carmell MA, Murchison EP, Alcorn H, et al. (2003) Dicer is essential for mouse development. Nat Genet 35: 215-217.

31. Muljo SA, Ansel KM, Kanellopoulou C, Livingston DM, Rao A, et al. (2005) Aberrant T cell differentiation in the absence of Dicer. J Exp Med 202: 261-269.

32. Elsarraj HS, Stecklein SR, Valdez K, Behbod F (2012) Emerging functions of microRNA-146a/b in development and breast cancer: microRNA-146a/b in development and breast cancer. J Mammary Gland Biol Neoplasia 17: 79-87.

33. Fujita PA, Rhead B, Zweig AS, Hinrichs AS, Karolchik D, et al. (2011) The UCSC Genome Browser database: update 2011. Nucleic Acids Res 39: D876-882.

34. Lewis BP, Shih IH, Jones-Rhoades MW, Bartel DP, Burge CB (2003) Prediction of mammalian microRNA targets. Cell 115: 787-798.

35. Lu LF, Boldin MP, Chaudhry A, Lin LL, Taganov KD, et al. (2010) Function of miR-146a in controlling Treg cell-mediated regulation of Th1 responses. Cell 142: 914-929.

36. Boldin MP, Taganov KD, Rao DS, Yang L, Zhao JL, et al. (2011) miR-146a is a significant brake on autoimmunity, myeloproliferation, and cancer in mice. J Exp Med 208: 1189-1201.

37. Dai L, Feng XR, Chen YP, Wen WQ, Xu YK (2008) [Imaging diagnosis of small hepatocellular carcinoma using ultrasound, contrast-enhanced ultrasound and multislice spiral CT]. Nan Fang Yi Ke Da Xue Xue Bao 28: 1469-1471.

38. He H, Jazdzewski K, Li W, Liyanarachchi S, Nagy R, et al. (2005) The role of microRNA genes in papillary thyroid carcinoma. Proc Natl Acad Sci U S A 102: 19075-19080.

39. Bockmeyer CL, Christgen M, Muller M, Fischer S, Ahrens P, et al. (2011) MicroRNA profiles of healthy basal and luminal mammary epithelial cells are distinct and reflected in different breast cancer subtypes. Breast Cancer Res Treat 130: 735-745.

40. Garcia AI, Buisson M, Bertrand P, Rimokh R, Rouleau E, et al. (2011) Down-regulation of BRCA1 expression by miR-146a and miR-146b-5p in triple negative sporadic breast cancers. EMBO Mol Med 3: 279-290.

41. Turner NC, Reis-Filho JS (2006) Basal-like breast cancer and the BRCA1 phenotype. Oncogene 25: 5846-5853.

42. Turner NC, Reis-Filho JS, Russell AM, Springall RJ, Ryder K, et al. (2007) BRCA1 dysfunction in sporadic basal-like breast cancer. Oncogene 26: 2126-2132.

43. Xia H, Qi Y, Ng SS, Chen X, Li D, et al. (2009) microRNA-146b inhibits glioma cell migration and invasion by targeting MMPs. Brain Res 1269: 158-165.

44. Hurst DR, Edmonds MD, Welch DR (2009) Metastamir: the field of metastasis-regulatory microRNA is spreading. Cancer Res 69: 7495-7498.

45. Bhaumik D, Scott GK, Schokrpur S, Patil CK, Campisi J, et al. (2008) Expression of microRNA-146 suppresses NF-kappaB activity with reduction of metastatic potential in breast cancer cells. Oncogene 27: 5643-5647.

46. Geraldo MV, Yamashita AS, Kimura ET (2012) MicroRNA miR-146b-5p regulates signal transduction of TGF-beta by repressing SMAD4 in thyroid cancer. Oncogene 31: 1910-1922.

47. Ghosh T, Soni K, Scaria V, Halimani M, Bhattacharjee C, et al. (2008) MicroRNA-mediated up-regulation of an alternatively polyadenylated variant of the mouse cytoplasmic {beta}-actin gene. Nucleic Acids Res 36: 6318-6332.

48. Vasudevan S, Tong Y, Steitz JA (2007) Switching from repression to activation: microRNAs can up-regulate translation. Science 318: 1931-1934.

49. Siegel PM, Muller WJ (2010) Transcription factor regulatory networks in mammary epithelial development and tumorigenesis. Oncogene 29: 2753-2759.

50. Bouras T, Pal B, Vaillant F, Harburg G, Asselin-Labat M-L, et al. (2008) Notch Signaling Regulates Mammary Stem Cell Function and Luminal Cell-Fate Commitment. Cell Stem Cell 3: 429-441.

51. Chapman RS, Lourenco PC, Tonner E, Flint DJ, Selbert S, et al. (1999) Suppression of epithelial apoptosis and delayed mammary gland involution in mice with a conditional knockout of Stat3. Genes Dev 13: 2604-2616.

52. Miranda KC, Huynh T, Tay Y, Ang YS, Tam WL, et al. (2006) A pattern-based method for the identification of MicroRNA binding sites and their corresponding heteroduplexes. Cell 126: 1203-1217.

53. Maritano D, Sugrue ML, Tininini S, Dewilde S, Strobl B, et al. (2004) The STAT3 isoforms alpha and beta have unique and specific functions. Nat Immunol 5: 401-409.

54. Flicek P, Amode MR, Barrell D, Beal K, Brent S, et al. (2012) Ensembl 2012. Nucleic Acids Res 40: D84-90.

55. Pruitt KD, Tatusova T, Maglott DR (2005) NCBI Reference Sequence (RefSeq): a curated non-redundant sequence database of genomes, transcripts and proteins. Nucleic Acids Res 33: D501-504.

56. Flanders KC, Wakefield LM (2009) Transforming growth factor-(beta)s and mammary gland involution; functional roles and implications for cancer progression. J Mammary Gland Biol Neoplasia 14: 131-144.

57. Floyd ZE, Segura BM, He F, Stephens JM (2007) Degradation of STAT5 proteins in 3T3-L1 adipocytes is induced by TNF-{alpha} and cycloheximide in a manner independent of STAT5A activation. Am J Physiol Endocrinol Metab 292: E461-468.

58. Sandberg R, Neilson JR, Sarma A, Sharp PA, Burge CB (2008) Proliferating cells express mRNAs with shortened 3' untranslated regions and fewer microRNA target sites. Science 320: 1643-1647.

59. Ji Z, Lee JY, Pan Z, Jiang B, Tian B (2009) Progressive lengthening of 3' untranslated regions of mRNAs by alternative polyadenylation during mouse embryonic development. Proc Natl Acad Sci U S A 106: 7028-7033.

60. Makeyev EV, Zhang J, Carrasco MA, Maniatis T (2007) The MicroRNA miR-124 promotes neuronal differentiation by triggering brain-specific alternative pre-mRNA splicing. Mol Cell 27: 435-448.

61. Boutz PL, Chawla G, Stoilov P, Black DL (2007) MicroRNAs regulate the expression of the alternative splicing factor nPTB during muscle development. Genes Dev 21: 71-84.

62. Levy DE, Lee CK (2002) What does Stat3 do? J Clin Invest 109: 1143-1148.

63. Orom UA, Kauppinen S, Lund AH (2006) LNA-modified oligonucleotides mediate specific inhibition of microRNA function. Gene 372: 137-141.

64. Caligioni CS (2009) Assessing reproductive status/stages in mice. Curr Protoc Neurosci Appendix 4: Appendix 4I.

65. Valdez KE, Fan F, Smith W, Allred DC, Medina D, et al. (2011) Human primary ductal carcinoma in situ (DCIS) subtype-specific pathology is preserved in a mouse intraductal (MIND) xenograft model. J Pathol 225: 565-573.